

1973

The crystal and molecular structures of $[\pi]$ - $C_5H_5Fe(CO)_3PF_6$ and two insecticides, dieldrin and endrin: an X-ray and neutron study of $K_2Sb_2(d-C_4H_2O_6)_2 \cdot 3H_2O$

Mary Edith Gress
Iowa State University

Follow this and additional works at: <https://lib.dr.iastate.edu/rtd>

 Part of the [Physical Chemistry Commons](#)

Recommended Citation

Gress, Mary Edith, "The crystal and molecular structures of $[\pi]$ - $C_5H_5Fe(CO)_3PF_6$ and two insecticides, dieldrin and endrin: an X-ray and neutron study of $K_2Sb_2(d-C_4H_2O_6)_2 \cdot 3H_2O$ " (1973). *Retrospective Theses and Dissertations*. 6199.
<https://lib.dr.iastate.edu/rtd/6199>

This Dissertation is brought to you for free and open access by the Iowa State University Capstones, Theses and Dissertations at Iowa State University Digital Repository. It has been accepted for inclusion in Retrospective Theses and Dissertations by an authorized administrator of Iowa State University Digital Repository. For more information, please contact digirep@iastate.edu.

INFORMATION TO USERS

This material was produced from a microfilm copy of the original document. While the most advanced technological means to photograph and reproduce this document have been used, the quality is heavily dependent upon the quality of the original submitted.

The following explanation of techniques is provided to help you understand markings or patterns which may appear on this reproduction.

1. The sign or "target" for pages apparently lacking from the document photographed is "Missing Page(s)". If it was possible to obtain the missing page(s) or section, they are spliced into the film along with adjacent pages. This may have necessitated cutting thru an image and duplicating adjacent pages to insure you complete continuity.
2. When an image on the film is obliterated with a large round black mark, it is an indication that the photographer suspected that the copy may have moved during exposure and thus cause a blurred image. You will find a good image of the page in the adjacent frame.
3. When a map, drawing or chart, etc., was part of the material being photographed the photographer followed a definite method in "sectioning" the material. It is customary to begin photoing at the upper left hand corner of a large sheet and to continue photoing from left to right in equal sections with a small overlap. If necessary, sectioning is continued again — beginning below the first row and continuing on until complete.
4. The majority of users indicate that the textual content is of greatest value, however, a somewhat higher quality reproduction could be made from "photographs" if essential to the understanding of the dissertation. Silver prints of "photographs" may be ordered at additional charge by writing the Order Department, giving the catalog number, title, author and specific pages you wish reproduced.
5. PLEASE NOTE: Some pages may have indistinct print. Filmed as received.

Xerox University Microfilms

300 North Zeeb Road
Ann Arbor, Michigan 48106

73-25,223

GRESS, Mary Edith, 1946-

THE CRYSTAL AND MOLECULAR STRUCTURES OF
 η -C₅H₅Fe(CO)₃PF₆ AND TWO INSECTICIDES, DIELDRIN
AND ENDRIN; AN X-RAY AND NEUTRON STUDY OF
K₂Sb₂(d-C₄H₂O₆)₂·3H₂O.

Iowa State University, Ph.D., 1973
Chemistry, physical

University Microfilms, A XEROX Company, Ann Arbor, Michigan

The crystal and molecular structures of $\pi\text{-C}_5\text{H}_5\text{Fe}(\text{CO})_3\text{PF}_6$
and two insecticides, dieldrin and endrin;
an X-ray and neutron study of $\text{K}_2\text{Sb}_2(\text{d-C}_4\text{H}_2\text{O}_6)_2 \cdot 3\text{H}_2\text{O}$

by

Mary Edith Gress

A Dissertation Submitted to the
Graduate Faculty in Partial Fulfillment of
The Requirements for the Degree of
DOCTOR OF PHILOSOPHY

Department: Chemistry
Major: Physical Chemistry

Approved:

Signature was redacted for privacy.

In Charge of Major Work

Signature was redacted for privacy.

For the Major Department

Signature was redacted for privacy.

For the Graduate College

Iowa State University
Ames, Iowa

1973

TABLE OF CONTENTS

	Page
INTRODUCTION	1
THE CRYSTAL AND MOLECULAR STRUCTURE OF π -C ₅ H ₅ Fe(CO) ₃ PF ₆ , A CATIONIC IRON CARBONYL COMPLEX	3
Introduction	3
Experimental	3
Solution and Refinement	5
Discussion	8
THE CRYSTAL AND MOLECULAR STRUCTURE OF THE INSECTICIDE ENDRIN	20
Introduction	20
Experimental	23
Solution and Refinement	26
Discussion	27
THE CRYSTAL AND MOLECULAR STRUCTURE OF THE INSECTICIDE DIELDRIN	43
Introduction	43
Experimental	45
Solution and Refinement	48
Supplementary Data and Refinement	53
Discussion	59

	Page
X-RAY AND WHITE RADIATION NEUTRON DIFFRACTION	
STUDIES OF OPTICALLY ACTIVE POTASSIUM ANTIMONY	
TARTRATE, $K_2Sb_2(\underline{d}\text{-C}_4\text{H}_2\text{O}_6)_2 \cdot 3\text{H}_2\text{O}$ (TARTAR EMETIC)	70
Introduction	70
Experimental	71
Solution and Refinement	77
Discussion	90
RESEARCH PROPOSALS	108
REFERENCES	112
ACKNOWLEDGEMENTS	117

INTRODUCTION

Four crystallographic structure determinations are presented in this thesis: those of dipotassium di- μ -d-tartrato(4)-bis(antimonate(III)) trihydrate, cyclopentadienyl iron tricarbonyl hexafluorophosphate, and the insecticides endrin and dieldrin. Each of the structures represents an interesting research problem, with the overall objective to learn the science and the art of crystallography.

The X-ray crystal structure determination of $K_2Sb_2(\underline{d}\text{-C}_4\text{H}_2\text{O}_6)_2 \cdot 3\text{H}_2\text{O}$ was undertaken as part of a continuing program in this laboratory to elucidate structure and bonding in antimony compounds, in particular, the lengthening of X-Sb-X bonds trans to one another and lone pair effects, if any. In addition, as a crystalline inorganic hydrate, the water molecules are very important in the overall crystal structure as ligands to metal ions and to minimize electrostatic repulsion between anions. To locate the hydrogen atoms and hydrogen bonding of water molecules in the crystal structure, a neutron diffraction study was carried out using the white radiation neutron diffraction technique.

The $\pi\text{-C}_5\text{H}_5\text{Fe}(\text{CO})_3\text{PF}_6$ structure determination is the first X-ray crystallographic study of a cationic iron carbonyl complex. The positively charged iron carbonyl

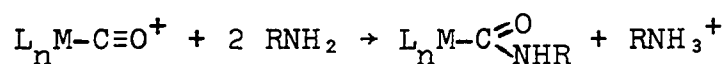
complex is compared with neutral iron carbonyl complexes and with the isoelectronic manganese species.

The cyclodiene insecticides endrin and dieldrin are geometrical isomers in which slight differences in structure appear to have a significant effect on biological activity. The structure determinations of endrin and dieldrin were more difficult crystallographic problems than the first two compounds, and were solved using direct methods. The exact solid state structural parameters are fundamental to toxicity studies of structure-activity relationships.

THE CRYSTAL AND MOLECULAR STRUCTURE OF $\pi\text{-C}_5\text{H}_5\text{Fe}(\text{CO})_3\text{PF}_6$,
A CATIONIC IRON CARBONYL COMPLEX

Introduction

Angelici and co-workers have extensively studied reactions of metal carbonyls with primary and secondary amines to form carboxamido complexes.¹⁻³



In particular, for iron cyclopentadienyl cations $[\text{C}_5\text{H}_5\text{Fe}(\text{CO})_2\text{L}^+]$ where $\text{L} = \text{CO}$ or $\text{P}(\text{C}_6\text{H}_5)_3$, they found that carboxamido complexes readily formed. In contrast, $\pi\text{-C}_5\text{H}_5\text{Mn}(\text{CO})_3$ which is isoelectronic with $\pi\text{-C}_5\text{H}_5\text{Fe}(\text{CO})_3^+$ will not react under the same conditions. We felt it would be worthwhile to carry out the structure investigation of $\pi\text{-C}_5\text{H}_5\text{Fe}(\text{CO})_3\text{PF}_6$ as this would be the first structure determination of an iron carbonyl cation and the results could be compared with those from the isoelectronic manganese species.

Experimental

Crystals of the compound were obtained from Dr. Angelici and their preparation is discussed elsewhere.¹ Preliminary examination via precession photographs exhibited mmm diffraction symmetry indicating an orthorhombic space group. Systematic absences for $0k\ell$: $k \neq 2n$, $h0\ell$: $\ell \neq 2n$

and $hk0$: $h \neq 2n$ uniquely determine the space group to be $Pbca$. The unit cell parameters obtained with chromium radiation ($K\alpha = 2.2909$, $K\beta = 2.0848\text{\AA}$) at 24°C are $\underline{a} = 15.235 \pm 0.009$, $\underline{b} = 12.672 \pm 0.005$, and $\underline{c} = 12.422 \pm 0.012\text{\AA}$. These parameters were obtained by a least squares fit⁴ of 14 2θ -values measured from zero-level Weissenberg films calibrated with superimposed aluminum powder lines ($a_0 = 4.0410\text{\AA}$). The calculated density of 1.93 g/cc for 8 molecules per cell agrees well with the observed density of $1.83 \pm 0.08 \text{ g/cc}$ determined by flotation techniques.

For data collection, a crystal of dimensions $0.30 \times 0.32 \times 0.32 \text{ mm}$ and nearly cubic in shape was mounted on the end of a glass fiber using Duco cement.

Intensity data were taken at room temperature (24°) using Zr-filtered Mo $K\alpha$ ($\lambda = 0.7107\text{\AA}$) radiation on a fully automated Hilger-Watts four-circle diffractometer equipped with a scintillation counter and interfaced to an SDS-910 computer in a real-time mode. One octant of data was collected within a theta sphere of 30° . Intensities were measured by counting at the peak center (θ_{hkl}) for ten seconds with two five second background counts at $\theta_{hkl} \pm (0.25 + (0.01 \times \theta_{hkl}))$. For conversion of peak height to integrated data, some integrated intensities were taken by the stepscan (moving crystal-moving counter) technique,⁵ and the integrated-peak height ratios were plotted as a

function of theta (0-30°). (No dependence on chi or phi was observed.) The intensities of three standard reflections which were re-measured periodically showed no decrease in intensity during data collection.

All intensity data were corrected for background and Lorentz-polarization effects. Because the linear absorption coefficient was small ($\mu = 15.2 \text{ cm}^{-1}$), no absorption correction was made. Minimum and maximum transmission factors were 0.61 and 0.63. Standard deviations (σ_I) in the intensities were estimated from the total count (TC) and background count (BC) values by $(\sigma_I)^2 = TC + BC + (0.05 \times TC)^2 + (0.05 \times BC)^2 + (0.05 \times I)^2$. The last three factors represent estimates for non-statistical errors in the total count, background count and the net intensity, respectively. The estimated standard deviation in the structure factor (σ_F) was found by the finite difference method.⁶ Of the 4175 reflections measured, 2662 had $F_o > 2.5 \sigma_F$ and were considered observed.

Solution and Refinement

The coordinates of the iron and phosphorus atoms were readily determined from an unsharpened Patterson map, and subsequent structure factor and electron density map calculations⁷ revealed the positions of the other atoms. The structure was refined by a full-matrix least-squares procedure using a local modification of Busing, Martin,

and Levy's OR FLS.⁸ The function minimized was $\Sigma\omega(|F_o|-|F_c|)^2$ where ω is the weight defined as $1/\sigma^2(F_o)$. Isotropic refinement resulted in a conventional discrepancy factor ($R = \Sigma||F_o|-|F_c||/\Sigma|F_o|$) of 0.154, and a weighted discrepancy factor ($\omega R = [\Sigma\omega(|F_o|-|F_c|)^2/\Sigma\omega|F_o|^2]^{1/2}$) of 0.214.

After conversion to anisotropic temperature factors, final convergence was reached at $R = 0.083$ and $\omega R = 0.111$, with the average shift/error for the last cycle of 0.04. A final electron density difference map showed no peaks greater than $1.1 \text{ e}^-/\text{\AA}^3$; there were some small peaks between fluorine atom positions, suggesting some rotational disorder of the PF_6 group.

Addition of hydrogen atom positions at calculated C-H distances of 1.07\AA and further refinement of the original structure resulted in $R = 0.082$ and $\omega R = 0.111$.

The relativistic Hartree-Fock scattering factors of Doyle and Turner⁹ for Fe^{+2} , P, F, O, and C were used, with those of iron and phosphorous modified for the real and imaginary parts of anomalous dispersion.¹⁰ Hydrogen scattering factors are from the tables by Hanson et al.¹¹ The final positional and thermal parameters and their standard deviations as derived from the inverse matrix of the final least squares cycle are given in Table 1. In Table 2 are listed the calculated positions of the hydrogen

Table 1. Final atomic coordinates and thermal parameters^a

Atom	x	y	z	β_{11}	β_{22}	β_{33}	β_{12}	β_{13}	β_{23}
Fe	0.13043(4) ^b	0.10282(5)	0.20710(6)	0.00328(3)	0.00464(5)	0.00591(5)	-0.00010(3)	-0.00012(3)	-0.00003(3)
P	0.41234(10)	0.24667(11)	0.04335(12)	0.00517(7)	0.00637(9)	0.00620(9)	-0.00033(6)	-0.00031(6)	0.00049(7)
P(1)	0.31169(40)	0.26715(68)	0.06988(63)	0.00631(27)	0.02903(103)	0.02124(79)	-0.00298(42)	0.00007(39)	0.00197(70)
P(2)	0.40268(76)	0.12625(40)	0.05398(51)	0.03033(101)	0.00677(32)	0.01293(54)	-0.00187(47)	-0.00283(60)	0.00008(33)
P(3)	0.01264(45)	0.22985(84)	0.47439(62)	0.00766(34)	0.03797(150)	0.01862(81)	0.00589(57)	-0.00356(39)	-0.00581(79)
P(4)	0.42523(65)	0.36658(40)	0.03427(48)	0.02515(89)	0.00731(33)	0.01273(50)	-0.00153(45)	0.00134(49)	0.00024(33)
P(5)	0.42709(39)	0.25105(41)	0.17063(36)	0.01202(38)	0.01419(48)	0.00697(28)	0.00052(34)	-0.00135(28)	-0.00034(30)
P(6)	0.39918(44)	0.25733(40)	0.41774(36)	0.01437(43)	0.01270(44)	0.00669(29)	-0.00057(36)	-0.00159(31)	0.00058(26)
O(1)	0.09838(47)	0.32932(39)	0.19661(47)	0.01012(39)	0.00519(29)	0.01690(66)	-0.00020(27)	-0.00135(39)	-0.00037(32)
O(2)	0.17060(41)	0.41128(51)	0.47587(37)	0.00812(32)	0.01585(61)	0.00592(32)	0.00041(33)	0.00087(26)	0.00118(31)
O(3)	0.44832(27)	0.03252(39)	0.31397(44)	0.00360(18)	0.00929(37)	0.01447(51)	-0.00106(20)	0.00069(23)	-0.00178(33)
C(1)	0.10855(45)	0.24241(44)	0.20005(52)	0.00599(29)	0.00514(33)	0.00938(51)	-0.00047(25)	-0.00013(37)	-0.00009(30)
C(2)	0.15460(42)	0.09397(49)	0.06300(50)	0.00541(28)	0.00804(43)	0.00650(39)	-0.00060(27)	-0.00018(27)	-0.00052(33)
C(3)	0.01693(36)	0.06215(46)	0.19108(46)	0.00395(22)	0.00604(33)	0.00800(42)	-0.00057(22)	-0.00021(24)	0.00077(30)
C(4)	0.24970(48)	0.11375(79)	0.28654(75)	0.00429(28)	0.01256(76)	0.01319(80)	-0.00141(37)	-0.00243(41)	0.00388(64)
C(5)	0.24283(59)	0.01811(95)	0.23710(67)	0.00696(43)	0.01720(107)	0.00906(58)	0.00719(60)	-0.00082(42)	0.00025(64)
C(6)	0.33144(78)	0.46627(55)	0.28306(79)	0.01133(67)	0.00595(42)	0.01452(91)	-0.00074(43)	0.00655(65)	0.00168(48)
C(7)	0.13538(53)	0.03338(89)	0.35893(62)	0.00685(41)	0.01615(97)	0.00772(53)	0.00072(50)	-0.00036(37)	0.00521(60)
C(8)	0.18542(71)	0.12173(65)	0.35947(69)	0.00962(58)	0.01000(61)	0.00985(66)	0.00088(48)	-0.00450(51)	-0.00175(49)

^aThe form of the anisotropic temperature factor expression is $\exp[-(\beta_{11}h^2 + \beta_{22}k^2 + \beta_{33}l^2 + 2\beta_{12}hk + 2\beta_{13}hl + 2\beta_{23}kl)]$.

^bIn this and in subsequent tables, estimated standard deviations are given in parentheses for the least significant figures.

Table 2. Calculated hydrogen atom positions^a

Atom	x	y	z
H(4) ^a	0.2978	0.1729	0.2697
H(5)	0.2858	-0.0106	0.1758
H(6)	0.1447	-0.1109	0.2617
H(7)	0.0784	0.0209	0.4091
H(8)	0.1755	0.1886	0.4121

^aThe hydrogen atoms are labeled according to the C atom to which they are bonded. For example, H(4) is bonded to C(4).

atoms in the cyclopentadienyl ring. Table 3 lists the observed and calculated structure factors. Interatomic distances and angles and their deviations as calculated using OR FFE¹² and the variance-covariance matrix from the final least squares cycle are given in Table 4. The computer drawings shown throughout the text were made using OR TEP.¹³

Discussion

Cyclopentadienyl iron tricarbonyl hexafluorophosphate exists as discrete $C_5H_5Fe(CO)_3^+$ and PF_6^- ions in the solid state. The coordination around the iron atom (Figure 1)

Table 4. Selected distances and angles and their estimated standard deviations for $\pi\text{-C}_5\text{H}_5\text{Fe}(\text{CO})_3\text{PF}_6$

(a) Distances (\AA)

Fe-C(1)	1.802(6)	P-F(1)	1.590(6)
Fe-C(2)	1.831(7)	P-F(2)	1.539(5)
Fe-C(3)	1.815(6)	P-F(3)	1.559(7)
C(1)-O(1)	1.113(7)	P-F(4)	1.536(5)
C(2)-O(2)	1.111(7)	P-F(5)	1.598(5)
C(3)-O(3)	1.112(7)	P-F(6)	1.574(5)
C(4)-C(5)	1.363(13)	Fe-C(4)	2.072(7)
C(5)-C(6)	1.428(14)	Fe-C(5)	2.055(6)
C(6)-C(7)	1.366(13)	Fe-C(6)	2.055(6)
C(7)-C(8)	1.355(13)	Fe-C(7)	2.083(7)
C(8)-C(4)	1.338(13)	Fe-C(8)	2.084(7)

(b) Angles (deg)

C(4)-C(5)-C(6)	106.9(7)	C(1)-Fe-C(2)	92.9(3)
C(5)-C(6)-C(7)	106.4(7)	C(2)-Fe-C(3)	93.8(3)
C(6)-C(7)-C(8)	108.0(8)	C(3)-Fe-C(1)	95.6(3)
C(7)-C(8)-C(9)	110.3(8)	Fe-C(1)-O(1)	177.3(7)
C(8)-C(9)-C(4)	108.4(7)	Fe-C(2)-O(2)	178.9(8)
		Fe-C(3)-O(3)	175.6(5)

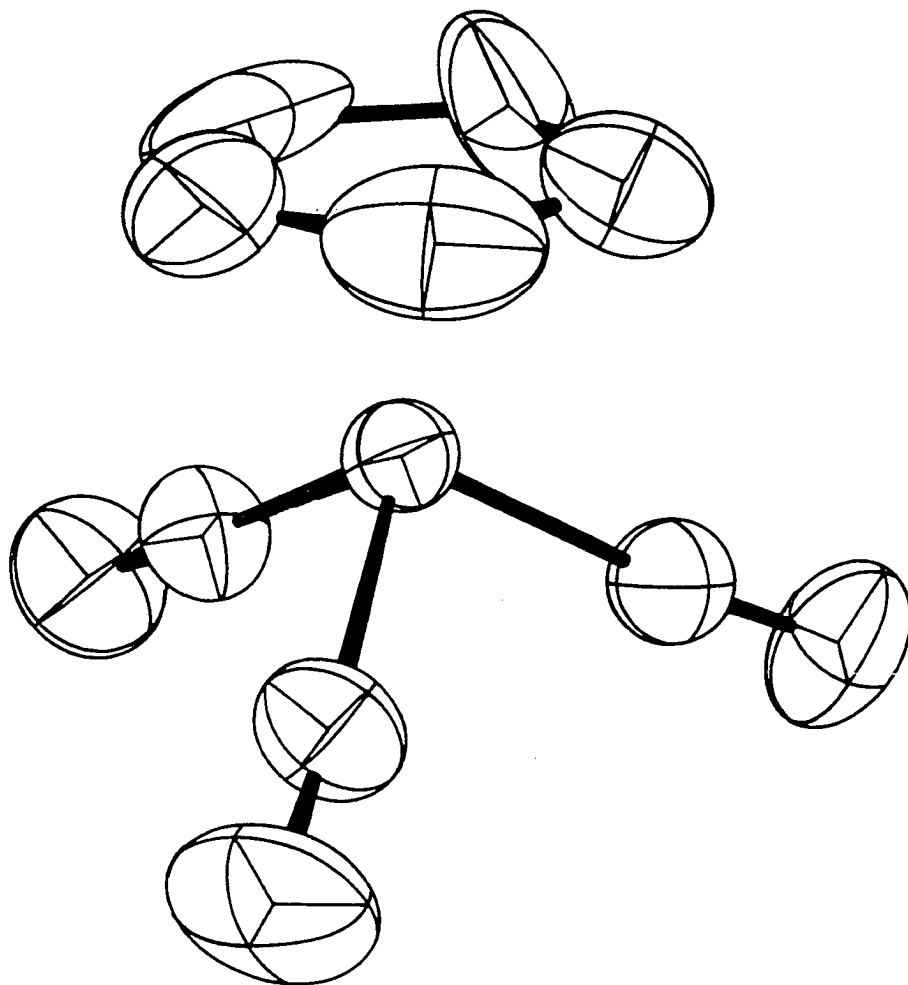


Figure 1. The $\pi\text{-C}_5\text{H}_5\text{Fe}(\text{CO})_3^+$ cation in $\pi\text{-C}_5\text{H}_5\text{Fe}(\text{CO})_3\text{PF}_6$

can best be described as octahedral with coordination to three carbonyl monodentate ligands and a $C_5H_5^-$ tridentate ligand. This configuration is in agreement with the current MO bonding scheme¹⁴ for this type of compound which uses primarily the d -orbitals on the metal and includes overlap of the e_1-d_{xy} and d_{yz} orbitals with C_5H_5 $e_1-\pi$ orbitals and involves back donation of the non-bonding d electrons into the $C\equiv O$ bond. The PF_6^- group, as expected, has approximately O_h symmetry, although as stated earlier, there exists some degree of rotational disorder in the solid.

A least squares plane was calculated for $C_5H_5^-$ to show its relationship to the plane described by the three carbonyl carbon atoms (Table 5). The two planes are essentially parallel with a dihedral angle of only 0.01° . A projection (Figure 2) of the cation normal to these planes shows the configuration of the carbonyl groups relative to the cyclopentadienyl ring. Note that one carbonyl carbon atom lies directly below a carbon atom of the ring, with the other two carbonyl carbon atoms at staggered positions. This implies that one orbital, involved in σ bonding to $C\equiv O$, will be directed toward the midpoint of a C-C bond in the ring. In two similar structures, $[\pi-C_5H_5Fe(CO)_2]_2C_4H_4$ ¹⁵ and $\pi-C_5H_5Fe(CO)_2C_4H_5SO_2$,¹⁶ it was also found that one monodentate ligand was directly below a cyclopentadienyl carbon atom.

Table 5. Planes involving ligand atoms^a

(i) Least Squares Plane of the Cyclopentadienyl Ring

$$\text{Equation: } 0.5911x - 0.4073y + 0.6962z - 4.1381 = 0$$

Distances of Atoms from the Plane:

Atom	Dev. (Å)
C(4)	-0.006
C(5)	0.004
C(6)	0.000
C(7)	-0.003
C(8)	0.006

(ii) Plane Defined by the Carbonyl Carbon Atoms

$$\text{Equation: } 0.5987x - 0.4009y + 0.6934z - 1.4772 = 0$$

^aPlane coordinates are defined relative to three orthogonal unit vectors along the a, b, and c directions.

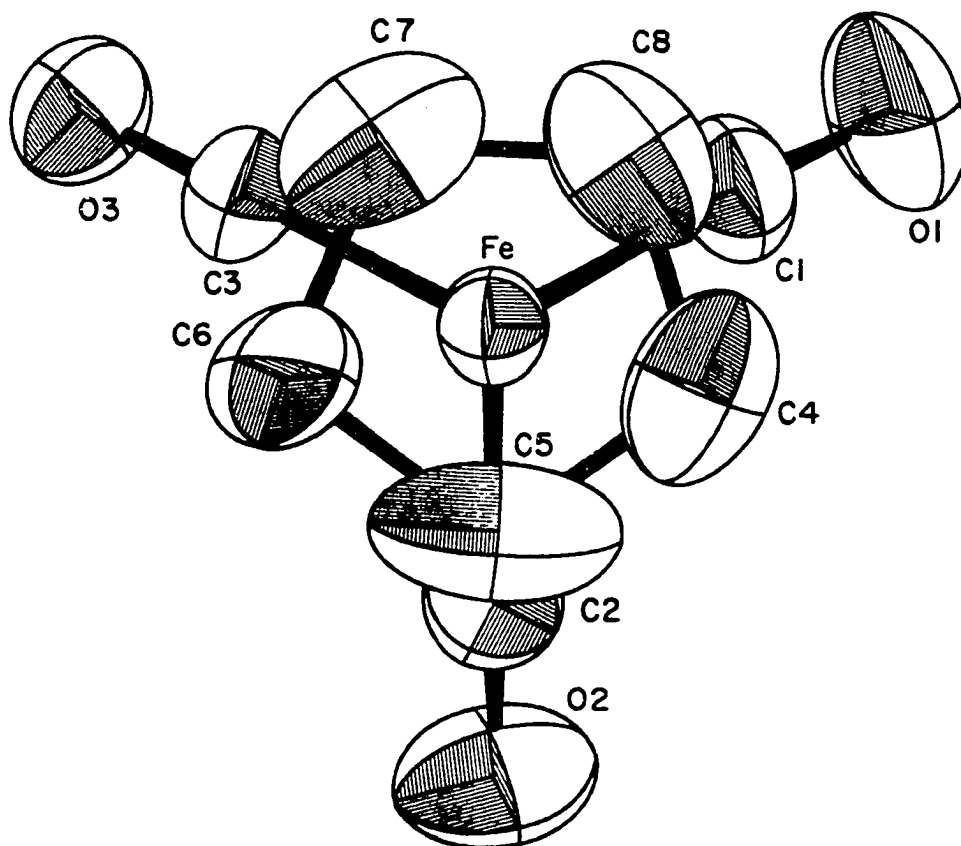


Figure 2. Projection of the $\pi\text{-C}_5\text{H}_5\text{Fe}(\text{CO})_3^+$ cation onto the cyclopentadienyl plane

The bonding of carbon monoxide ligands has been characterized in numerous compounds as sigma donation of electron density from the carbon atom accompanied by back donation of electron density from non-bonding metal orbitals into the $C\equiv O \pi^*$ orbitals. Structural data for a variety of iron carbonyl complexes are summarized in Table 6. A comparison of bond lengths given in this table shows that the C-O distances in $\pi-C_5H_5Fe(CO)_3PF_6$ are the shortest found (1.111(7), 1.112(7), and 1.113(7)Å) and the Fe-C(carbonyl) distances are the longest found (1.802(6), 1.815(6), and 1.831(7)Å). Brown and Darensbourg¹⁷ in IR studies of metal carbonyls have shown that for the series $V(CO)_6^-$, $Cr(CO)_6$, and $Mn(CO)_6^+$ the carbon-oxygen stretching frequency increases with higher positive charge on the metal ion. Force constants calculated from C-O stretching frequencies of Fe, Mn, and Re carbonyl compounds are usually higher when the metal is formally positively charged.³ The short C-O distances found in this study agree quite well with these observations.

The C-Fe-C angles appear consistent with other iron carbonyls, as is the deviation from linear Fe-C-O bonds. Kettle¹⁸ has shown that there is no symmetry requirement that the two $C\equiv O \pi$ bonds interact equally with the metal orbitals, so that linear bonds are not necessarily expected.

As in most other metal π -bonded cyclopentadienyl complexes there is some variation in the carbon-carbon bond lengths in the cyclopentadienyl ligand. It has been suggested¹⁹⁻²¹ that the non-equivalent bond distances are indicative of localization of electron density, and that there is unequal overlap of d_{yz} and d_{xz} metal orbitals with the e MO's of C_5H_5 . In the present study (with variations greater than standard deviations) this appears to be the case. Carbon atoms forming the shortest Fe-C bonds in general exhibit the longest C-C distances. For example, the shortest Fe-C distances are Fe-C(5) and Fe-C(6), both 2.055(6) \AA , and the longest C-C distance in the cyclopentadienyl ring is C(5)-C(6) (1.428 \AA).

An X-ray crystal study of $\pi-C_5H_5Mn(CO)_3$ was carried out by Berndt and Marsh in 1962.²² The molecular configuration is basically the same as found for the cation in the present study. However, carbon-oxygen bond distances (1.129, 1.142, 1.131 \AA) are longer, probably due to increased back donation of electron density from the neutral Mn compared to the positively charged Fe atom. The C-Mn-C angles are 91, 91, and 94 $^\circ$ and the Mn-C-O bond angles are 176, 178, and 180 $^\circ$. The other major difference between the two structures is a 12 $^\circ$ rotation of the carbon monoxide ligands relative to the cyclopentadienyl ring. This transition, a 12 $^\circ$ rotation, which may or may not be the

Table 6. Comparison of structural results for iron carbonyl complexes

	C-O bond lengths (Å)	Average Fe-C bond lengths (Å)	Fe-C-O bond angles (degrees)	C-Fe-C bond angles (degrees)
$\text{CH}_3\text{SF}_2(\text{CO})_6 \cdot \frac{1}{2} \text{S}^{\text{a}}$	1.17(2), 1.16(2), 1.20(2), 1.14(3) 1.23(2), 1.17(2), 1.19(2), 1.17(2) 1.17(2), 1.16(2), 1.20(2), 1.20(2)	1.74(2)	174(2), 173(2), 178(2), 177(2), 176(2), 176(2), 174(2), 177(2), 177(2), 175(2), 175(2), 175(2)	98(1), 98(1), 99(1), 103(1), 98(1), 97(1), 98(1), 95(1), 88(1), 91(1), 91(1), 91(1)
$[\text{Fe}(\text{A}^{\text{c}}-\text{C}_5\text{H}_5)(\text{CO})(\text{SC}_2\text{H}_3)_2\text{BF}_4]^{\text{c}}$	1.16(2)	1.79(2)		
$[\text{n-C}_5\text{H}_5\text{Fe}(\text{CO})_2\text{C}_4\text{H}_4]^{\text{d}}$	1.143(8), 1.146(9)	1.75(1)	178.2(7), 179.7(6)	86.0(3), 90.6(3), 94.1(3), 89.3(6)
(Vitamin-A aldehyde)tricarbonyliron ^e	1.15(2), 1.16(2), 1.15(2)	1.78(2)	176(2), 177(2), 178(2)	90(1), 101(1), 105(1)
$\text{Fe}_2(\text{CO})_6(\text{C}_6\text{H}_5\text{C}_2\text{H}_4)_3^{\text{e}}$	1.142(16), 1.151(17), 1.144(20), 1.167(17), 1.159(17)	1.77(2)	176.0(12), 176.8(12), 176.4(13), 174.4(12), 180.0(12)	98.6(6), 91.9(6), 94.8(6)
$\text{n-C}_5\text{H}_5\text{Fe}(\text{CO})_2\text{Mn}(\text{CO})_5^{\text{f}}$	1.169(23) (Av.)	1.72(3)	170(2), 173(2), 174(2), 174(2)	94.9(11), 94.7(11)
$\text{n-C}_5\text{H}_5\text{Fe}(\text{CO})_2\text{C}_4\text{H}_5\text{SO}_2^{\text{g}}$	1.129(14) (Av.)	1.78(1)	174.2(10), 178.8(10)	93.0(4), 88.9(4), 96.1(5)
$\text{n-C}_5\text{H}_5\text{Fe}(\text{CO})_2(\text{n-C}_5\text{H}_5)^{\text{h}}$	1.16(2), 1.15(3)	1.70(2)	174(2), 174(2)	89(1), 92(1), 96(1)
$\text{n-C}_5\text{H}_5\text{Fe}(\text{CO})_3\text{PF}_6^{\text{i}}$	1.113(7), 1.112(7), 1.111(7)	1.82(1)	175.6(5), 177.3(7), 178.9(8)	95.6(3), 93.8(3), 92.9(3)

^aReference 23.

^bReference 24.

^cReference 15.

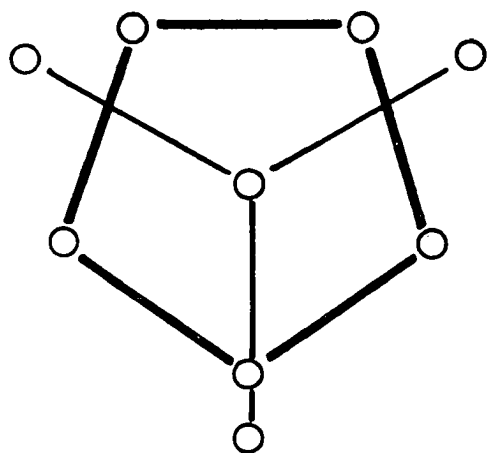
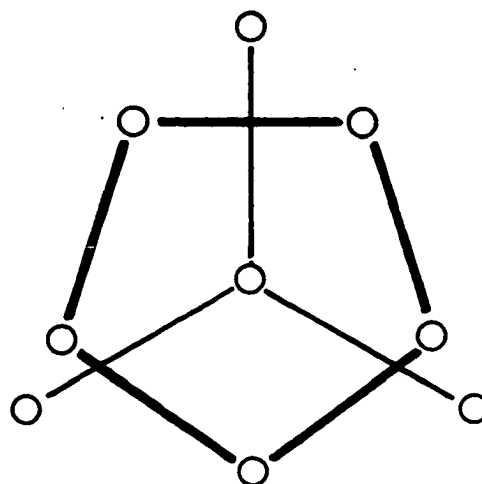
^dReference 25.

^eReference 26.

^fReference 27.

^gReference 28.

^hReference 29.

 $\pi\text{-C}_5\text{H}_5\text{Fe}(\text{CO})_3^+$  $\pi\text{-C}_5\text{H}_5\text{Mn}(\text{CO})_3$

result of packing forces in the crystal, gives the two compounds different geometrical configurations, but it would be difficult to say whether this would affect their relative reactivities.

THE CRYSTAL AND MOLECULAR STRUCTURE OF THE
INSECTICIDE ENDRIN

Introduction

Endrin is one of several highly toxic cyclodiene insecticides. The cyclodiene insecticides, a group which also includes dieldrin, isodrin, aldrin, heptachlor, chlordane, and telodrin, are highly chlorinated cyclic hydrocarbons named "cyclodiene" because of their preparation from cyclopentadiene.²⁹

These compounds are very similar to one another (for example, endrin and dieldrin, $C_{12}H_8Cl_6O$, are geometrical isomers) and yet slight differences in their structures appear to greatly affect their activity. These differences are illustrated in Table 7 which lists the toxicity (LD_{50}

Table 7. Toxicities of several cyclodiene insecticides^a

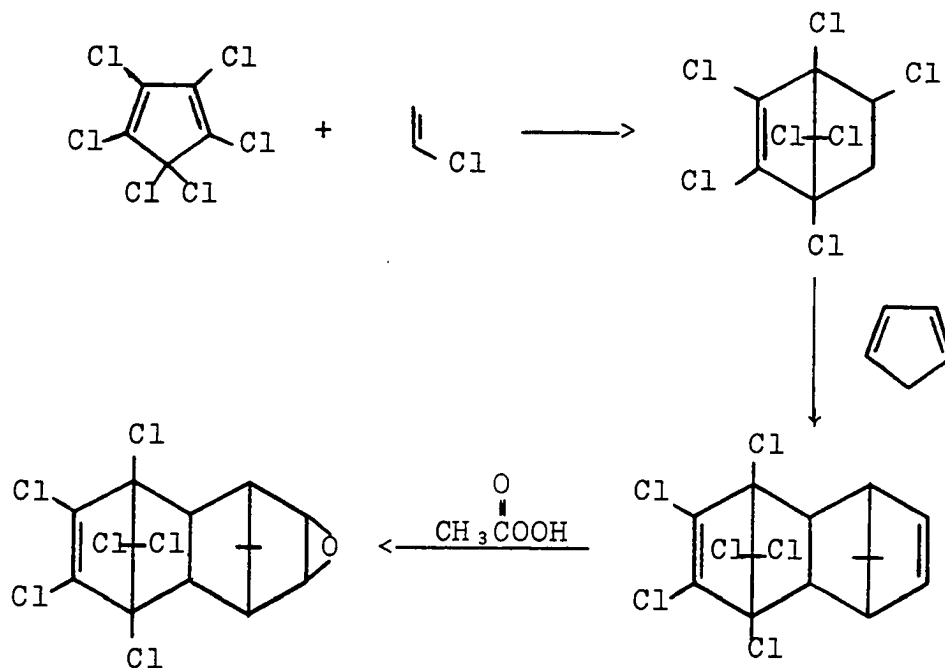
Compound	Housefly topical LD_{50} $\mu\text{g/g}$	Rat oral LD_{50} mg/kg
Endrin	3.0	7.5-7.8
Dieldrin	0.9	46
Aldrin	3.0	39-60
Heptachlor	2.2	100-162
Alodan	10.0	1500
Telodrin	1.1	4.8-5.5

^aThis table was taken in part from R. L. Metcalf's "The Chemistry and Biology of Pesticides," p. 91 (Reference 30).

is the lethal dose for one-half the population) of several cyclodiene insecticides to houseflies and rats.³⁰ On consultation with P. A. Dahm, Department of Zoology and Entomology, it was found that relatively little work has been done relating molecular structure to toxic activity of these compounds.

The poisoning of insects by cyclodiene insecticides is thought to occur in the ganglia of the central nervous system³⁰ although the exact mechanism of action is unknown. Soloway³¹ has shown there is correlation between molecular structure and biological activity of cyclodiene insecticides. In a series of tests of different cyclodiene compounds on several classes of insects, he has found that highly toxic cyclodiene compounds have several characteristics in common. These are the presence of two electronegative centers similarly positioned in the molecule (a polychlorinated center and another electronegative center such as Cl, O, S, or a double bond) which presumably can become attached to a biological site, a mirror plane through the dichloromethano bridge so that the electronegative centers are equally positioned across the mirror, and an overall similarity to one another in shape and size. Other cyclodiene compounds showed little or no toxic properties.

Endrin may be prepared by the Diels-Alder reactions²⁹



which should yield the endo-endo isomer, 1,2,3,4,10,10-hexachloro-6,7-epoxy-1,4,4a,5,6,7,8,8a-octahydro-endo-endo-1,4:5,8-dimethanonaphthalene. It should be noted that the structural formula is commonly written either endo-endo^{30,32,33} or exo-exo.^{34,35} This appears to be primarily a difference in American and British conventions and should not imply that there is any question about the relative orientation of the two norbornene rings.

The position of the epoxide ring, however, whether it is exo or endo to the non-chlorinated norbornene ring, is not defined. In this crystal structure determination we hoped to obtain the orientation of the epoxide ring and

also to provide accurate atomic coordinates in the molecule for use in model building in structure-activity studies of cyclodiene insecticides.

Experimental

Crystals of the compound were kindly supplied by P. A. Dahm. The crystals were clear and colorless with sharply defined faces. The crystals, although air-stable, were found to decompose upon exposure to X-rays, and it was found that mounting the crystals in thin-walled Lindemann glass capillaries retarded this decomposition. Preliminary precession photographs exhibited mmm diffraction symmetry. The systematic alternate extinctions along the three axes, $h,0,0: h \neq 2n$, $0,k,0: k \neq 2n$, and $0,0,l: l \neq 2n$ uniquely determined the orthorhombic space group $P2_12_12_1$. The unit cell parameters at 24°C are $a=15.273(2)$, $b=11.508(2)$, and $c=8.202(1)\text{\AA}$. These parameters and their standard deviations were obtained by a least-squares fit to 12 independent reflection angles⁴ whose centers were determined by left-right, top-bottom beam splitting on a previously aligned Hilger-Watts four-circle diffractometer (Cu K α radiation, $\lambda=1.5418\text{\AA}$). Any error in the instrumental zero was eliminated by centering the reflection at both +2 θ and -2 θ . A calculated density of 1.756 g/cc for four molecules per unit cell agrees well with the observed density 1.75 g/cc which was determined by flotation techniques.

For data collection, a crystal with dimensions 0.20 x 0.12 x 0.12 mm was sealed in a thin-walled Lindemann glass capillary with the a axis coincident with the spindle axis. Intensity data were taken at room temperature (24°) using Ni-filtered Cu K α ($\lambda=1.5418\text{\AA}$) radiation on a fully automated Hilger-Watts four-circle diffractometer equipped with a scintillation counter and interfaced to an SDS-910 computer in a real-time mode. Intensities were measured within one octant of a theta sphere of 55°, and were measured by counting at the peak center (θ_{hkl}) for ten seconds with two five second background counts at $\theta_{hkl} \pm (0.25 + (0.01 \times \theta_{hkl}))$. For conversion of peak height to integrated data, some integrated intensities were taken by the stepscan (moving crystal-moving counter) technique.⁵ No dependence on chi or phi was observed, and the integrated-peak height ratios were plotted as a function of theta. A total of 1022 independent reflections were recorded in this manner.

As a check on electronic and crystal stability, three standard reflections were measured periodically during data collection. The standard reflections indicated appreciable decomposition of the crystal, with the total decrease being about 25%. Decomposition curves drawn using the three standard reflections showed discontinuities at time periods where data collection had been stopped indicating that

decomposition occurred during and continued after exposure to X-rays. In later refinement of the structure it was found that using three scale factors gave better refinement of the structure than scaling each reflection for decomposition.

The intensity data were corrected for background and Lorentz-polarization effects, with an appropriate correction factor for peak height-integrated data. The absorption coefficient (μ) is 108 cm^{-1} . An absorption correction was made using the Tompa-Alcock absorption correction program.^{36,37} The maximum and minimum transmission factors were respectively, 37.5 and 27.7%. Standard deviations (σ_I) in the intensities were calculated by

$$(\sigma_I)^2 = [\text{TC} + \text{BC} + (0.05 \times \text{TC})^2 + (0.05 \times \text{BC})^2 + (0.05 \times \text{NET})^2] / A^2$$

where TC, BC, NET, and A are the total count, background count, net count, and transmission factor, respectively. The quantities 0.05 represent estimates for non-statistical errors in the total count, background count, and absorption correction, respectively. Values for σ_{F_o} were obtained from σ_I by the finite difference method.⁶ Of the 1022 measured intensities, 866 had $F_o > 2.5\sigma_{F_o}$ and were considered observed.

Solution and Refinement

The structure was solved using the MULTAN programs of Main, et al.³⁸ The chlorine atom positions were located by an E-map based on 166 reflections with $E > 1.25$, with the phases determined by application of the tangent formula of Karle and Hauptman.³⁹ The light atoms were readily located by an electron density calculation phased by the chlorine atoms.

The structure was refined by a full-matrix least-squares procedure using a local modification of Busing, Martin, and Levy's OR FLS.⁸ The function minimized was $\sum \omega (|F_o| - |F_c|)^2$ where ω is the weight defined as $1/\sigma^2(F_o)$. Isotropic refinement with the three scale factors resulted in a conventional discrepancy factor ($R = \sum ||F_o| - |F_c|| / \sum |F_o|$) of 0.194, and a weighted discrepancy factor ($\omega R = [\sum \omega (|F_o| - |F_c|)^2 / \sum \omega |F_o|^2]^{\frac{1}{2}}$) of 0.231. The scattering factors are from the tables by Hanson, Herman, Lea, and Skillman.¹¹

Two sets of 10 reflections with apparent angle-setting errors associated with them were removed from the data set. Further refinement of the structure with anisotropic temperature factors and 846 reflections resulted in $R=0.107$ and $\omega R=0.124$, with the average shift/error for the last cycle of 0.01. Due to the decomposition problem it was

felt that the data were not good enough to justify inclusion of hydrogen atoms in the refinement. A final electron density difference map showed no peaks higher than $0.7e^-/\text{\AA}^3$.

The final values of the positional parameters are given in Table 8 and anisotropic thermal parameters in Table 9 with standard deviations as derived from the inverse matrix. The observed and calculated structure factors are given in Table 10. Interatomic distances and angles and their deviations were calculated using ORFFE¹² and the variance-covariance matrix from the last least squares cycle. These are given in Table 11.

Discussion

The crystallographic study of endrin (Figure 3) confirms the endo-endo configuration of the molecule. The epoxide group is exo with respect to the non-chlorinated norbornene ring. The structural formula should be written 1,2,3,4,10,10-hexachloro-exo-6,7-epoxy-1,4,4a,5,6,7,8,8a-octahydro-endo-endo-1,4:5,8-dimethanonaphthalene.

Bond distances and angles (Table 11), in general, do appear to be significantly different than those used by Soloway³¹ to build Courtauld models of cyclodiene insecticides. These differences (longer carbon-carbon single bonds and some different angles) are due to strain in the heterocyclic system.

Table 8. Final positional parameters ($\times 10^4$) for endrin

Atom	x	y	z
C1(1)	9214(4)	8840(6)	2828(7)
C1(2)	9389(5)	6005(6)	2945(9)
C1(3)	7778(5)	4913(6)	5391(10)
C1(4)	6588(4)	7073(8)	6713(9)
C1(5)	7377(5)	9650(6)	5093(8)
C1(6)	7124(4)	7847(6)	2781(8)
C(1)	8735(13)	8081(18)	4395(24)
C(2)	8708(15)	6709(18)	4185(26)
C(3)	8090(18)	6300(21)	5166(27)
C(4)	7609(14)	7321(28)	5946(34)
C(5)	8227(16)	7960(20)	7248(31)
C(6)	8769(16)	7329(22)	8657(27)
C(7)	9224(17)	6253(18)	7946(29)
C(8)	-67(15)	6684(27)	6844(35)
C(9)	9872(12)	7982(23)	6970(29)
C(10)	9014(14)	8404(20)	6126(27)
C(11)	7717(14)	8255(16)	4545(28)
C(12)	9577(17)	8192(21)	8825(29)
O	1567(11)	6163(17)	8459(21)

Table 9. Final anisotropic thermal parameters ($\times 10^4$) for endrin^a

Atom	β_{11}	β_{22}	β_{33}	β_{12}	β_{13}	β_{23}
C1(1)	43(3)	141(6)	159(11)	-28(4)	6(5)	24(8)
C1(2)	64(4)	141(7)	213(13)	32(4)	0(6)	-50(9)
C1(3)	77(5)	102(6)	338(18)	-29(5)	-26(8)	4(9)
C1(4)	30(3)	226(10)	237(13)	-15(4)	21(5)	41(10)
C1(5)	66(4)	136(8)	209(12)	49(4)	-1(6)	1(8)
C1(6)	36(3)	163(7)	181(11)	-5(4)	-16(5)	13(8)
C(1)	27(9)	95(20)	112(32)	-12(11)	-1(14)	15(22)
C(2)	46(12)	78(19)	137(37)	28(12)	-14(18)	-2(23)
C(3)	75(17)	102(22)	132(37)	-13(15)	19(23)	-5(27)

^aThe form of the anisotropic temperature factor expression is $\exp[-(\beta_{11}h^2 + \beta_{22}k^2 + \beta_{33}l^2 + 2\beta_{12}hk + 2\beta_{13}hl + 2\beta_{23}kl)]$.

Table 9 (Continued)

Atom	β_{11}	β_{22}	β_{33}	β_{12}	β_{13}	β_{23}
C(4)	21(11)	213(35)	223(48)	19(16)	-1(19)	5(41)
C(5)	45(12)	108(22)	209(45)	9(13)	-41(20)	7(29)
C(6)	52(14)	125(25)	141(36)	1(15)	4(18)	-27(28)
C(7)	64(15)	70(18)	199(42)	14(14)	-10(22)	18(28)
C(8)	25(11)	185(37)	233(56)	16(15)	-18(21)	60(39)
C(9)	13(8)	141(27)	165(38)	0(11)	-24(15)	37(30)
C(10)	38(11)	120(24)	160(38)	-58(13)	-4(18)	21(26)
C(11)	34(10)	60(15)	197(42)	-6(10)	-22(18)	28(22)
C(12)	59(14)	116(23)	153(38)	3(16)	10(21)	-32(27)
O	44(9)	136(17)	232(34)	21(10)	-25(14)	14(23)

Table 11. Selected bond distances and angles for endrin

(a) Distances (Å)

C(1)-C(2)	1.60(3)	C(8)-C(9)	1.51(4)
C(2)-C(3)	1.32(3)	C(9)-C(10)	1.55(3)
C(3)-C(4)	1.53(4)	C(6)-C(12)	1.59(4)
C(4)-C(5)	1.59(3)	C(9)-C(12)	1.58(3)
C(5)-C(10)	1.58(3)	C(7)-O	1.48(3)
C(10)-C(1)	1.51(3)	C(8)-O	1.48(3)
C(4)-C(11)	1.58(3)	C(1)-Cl(1)	1.71(2)
C(1)-C(11)	1.56(3)	C(2)-Cl(2)	1.66(2)
C(5)-C(6)	1.58(3)	C(3)-Cl(3)	1.69(2)
C(6)-C(7)	1.54(3)	C(4)-Cl(4)	1.69(2)
C(7)-C(8)	1.48(4)	C(11)-Cl(5)	1.75(2)
		C(11)-Cl(6)	1.75(2)

(b) Angles (deg)

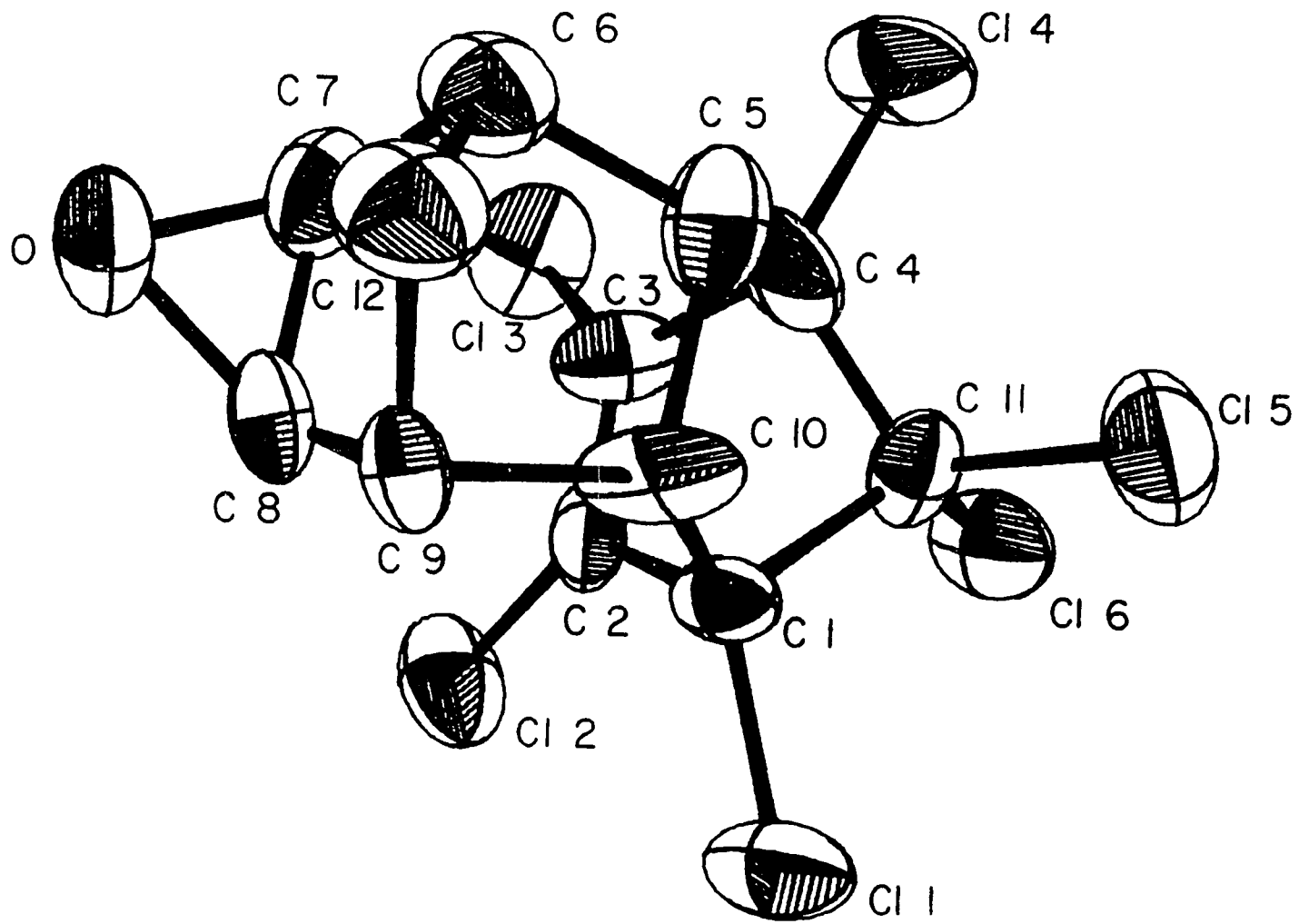
C(1)-C(2)-C(3)	108(2)	C(6)-C(12)-C(9)	92(2)
C(2)-C(3)-C(4)	108(2)	O-C(7)-C(8)	60(1)
C(3)-C(4)-C(5)	111(2)	C(7)-C(8)-O	60(1)
C(4)-C(5)-C(10)	102(2)	C(7)-O-C(8)	60(1)
C(5)-C(10)-C(1)	104(1)	C(1)-C(10)-C(9)	124(2)
C(10)-C(1)-C(2)	111(2)	C(4)-C(5)-C(6)	124(2)

Table 11 (Continued)

(b) Angles (deg)

C(3)-C(4)-C(11)	101(2)	C(2)-C(3)-C1(3)	127(2)
C(5)-C(4)-C(11)	95(2)	C(4)-C(3)-C1(3)	124(2)
C(2)-C(1)-C(11)	96(2)	C(3)-C(4)-C1(4)	117(2)
C(10)-C(1)-C(11)	100(2)	C(5)-C(4)-C1(4)	112(2)
C(1)-C(11)-C(4)	94(2)	C(1)-C(2)-C1(2)	123(2)
C(5)-C(6)-C(7)	110(2)	C(3)-C(2)-C1(2)	129(2)
C(6)-C(7)-C(8)	106(2)	C(10)-C(1)-C1(1)	116(1)
C(7)-C(8)-C(9)	105(2)	C(2)-C(1)-C1(1)	116(2)
C(8)-C(9)-C(10)	110(2)	C(11)-C(4)-C1(4)	118(2)
C(9)-C(10)-C(5)	106(2)	C(11)-C(1)-C1(1)	114(1)
C(10)-C(5)-C(6)	100(2)	C(1)-C(11)-C1(6)	114(2)
C(5)-C(6)-C(12)	100(2)	C(1)-C(11)-C1(5)	108(1)
C(7)-C(6)-C(12)	101(2)	C(4)-C(11)-C1(6)	110(1)
C(10)-C(9)-C(12)	98(2)	C(4)-C(11)-C1(5)	115(2)
C(8)-C(9)-C(12)	104(2)	C1(5)-C(11)-C1(6)	115(1)

Figure 3. View of the endrin molecule, 1,2,3,4,10,10-hexachloro-exo-6,7-epoxy-1,4,4a,5,6,7,8,8a-octahydro-endo-endo-1,4:5,8-dimethano-naphthalene

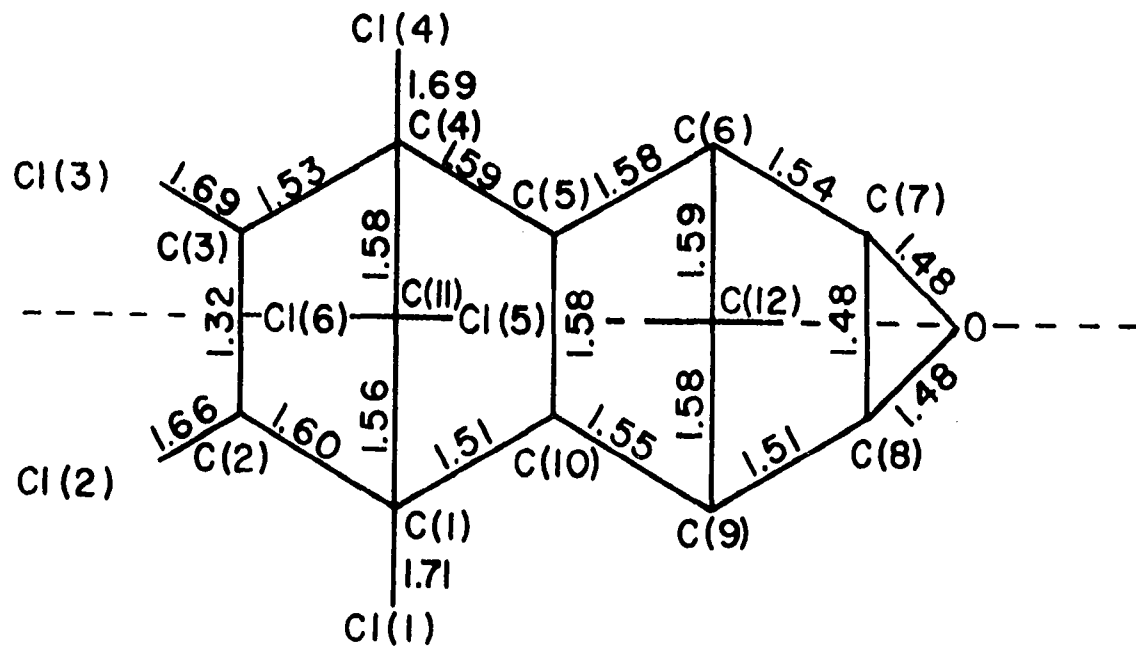


An approximate non-crystallographic mirror plane bisects the molecule through the methano bridge carbon atoms. Bond distances on either side of the mirror (Figure 4) are the same, within standard deviations, with the exception of C(1)-C(2) and C(3)-C(4) which are 1.60 and 1.53Å, and C(1)-C(10) and C(4)-C(5) which are 1.51 and 1.59Å, respectively. This slight distortion of the chlorinated norbornene part of the molecule also occurs in a similar compound, photoaldrin, the crystal structure of which was determined by Khan, Baur, and Khan in 1972.⁴⁰ In the photoaldrin structure these distances are 1.62 and 1.54Å and 1.51 and 1.60Å.

Other comparable bond distances in endrin and photoaldrin are very nearly the same. Carbon-carbon single bond lengths are observed, as in other strained heterocyclic systems, to be lengthened from the normal 1.54Å. The average C-C single bond in endrin is 1.56Å, and in photoaldrin, 1.57Å.

The carbon-carbon double bond length (1.32(3)Å) and epoxide C-O bond distances (1.48(3) and 1.48(3)Å) are typical for medium sized organic molecules. The methano bridge C-Cl distances are 1.75(2) and 1.75(2)Å which are normal C-Cl distances, although the other C-Cl distances, 1.71(2), 1.66(2), 1.69(2), and 1.69(2)Å, appear to be somewhat short.

Figure 4. Bond distances in the endrin molecule. The mirror plane is non-crystallographic



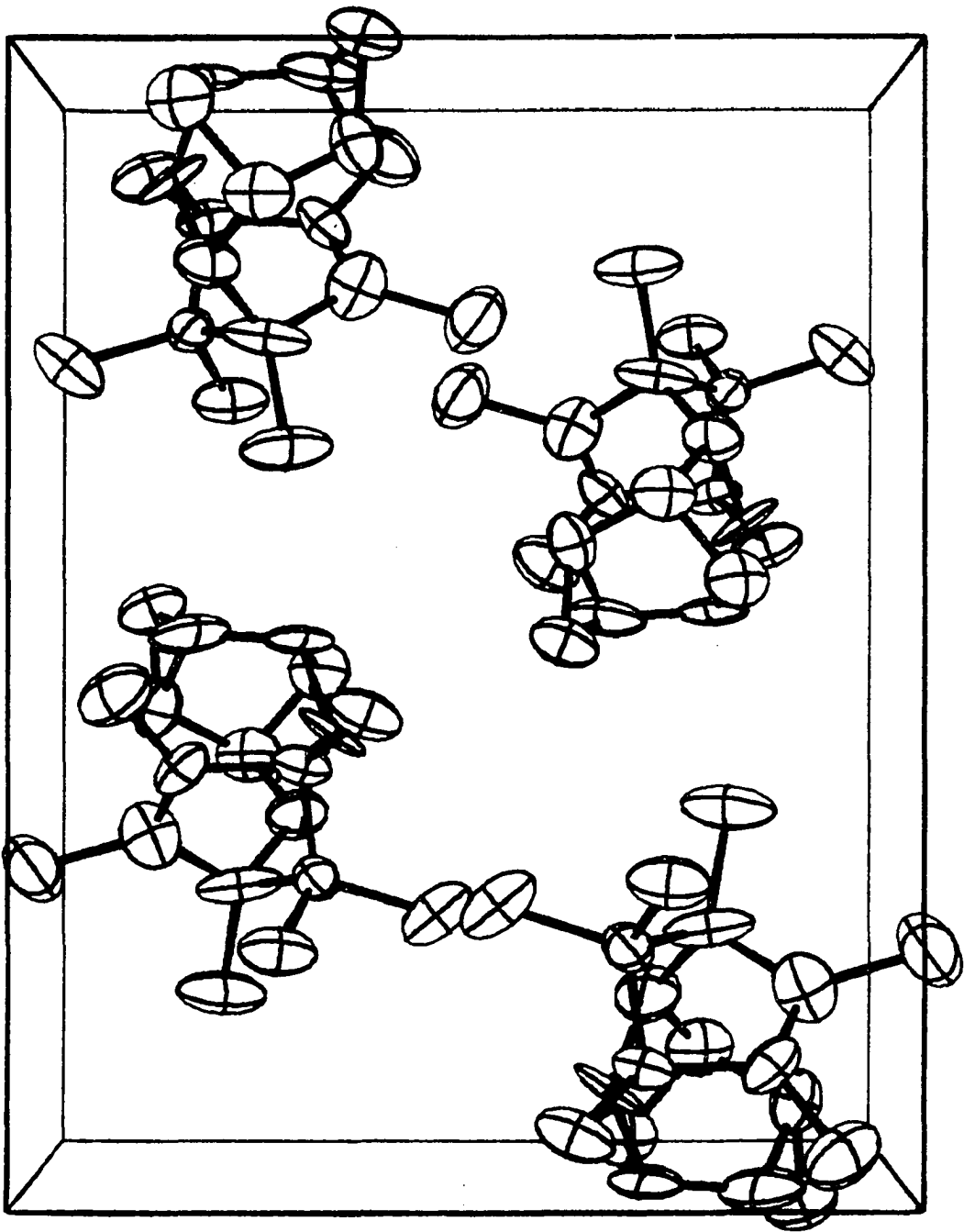
Bond angles are also mirrored across the non-crystallographic mirror plane within standard deviations, with the exception of the angles associated with the slightly distorted chlorinated norbornene ring mentioned above. These are C(3)-C(4)-C(11) (101°) and C(5)-C(4)-C(11) (95°), and C(2)-C(1)-C(11) (96°) and C(10)-C(1)-C(11) (100°). The methano bridge C-C-C angles, C(1)-C(11)-C(4) and C(6)-C(12)-C(9), are 94° and 92° , respectively.

The longest dimension across the mirror plane is 5.47\AA (the Cl(1)-Cl(4) distance) and the length of the molecule, from the epoxide oxygen to a bridgehead chlorine, Cl(6), is 6.78\AA .

A unit cell drawing of endrin is shown in Figure 5. Of the calculated intermolecular distances, there is only one distance which might be considered significantly less than the sum of the van der Waal radii. This is the distance between C(12) and Cl(1) of the adjacent molecule in the c direction, 3.37\AA . Weak hydrogen bonds, C-H...Cl bonds, may connect molecules in infinite chains in the c-direction.

After this crystal structure investigation had been completed, an X-ray crystallographic structure determination of endrin was reported in J. Chem. Soc.⁴¹ by T. P. DeLacy and C. H. L. Kennard of the Department of Chemistry, University of Queensland, Australia. Their

Figure 5. A unit cell drawing of endrin. The a-axis is across the page from left to right, b is up, and c is looking into the page



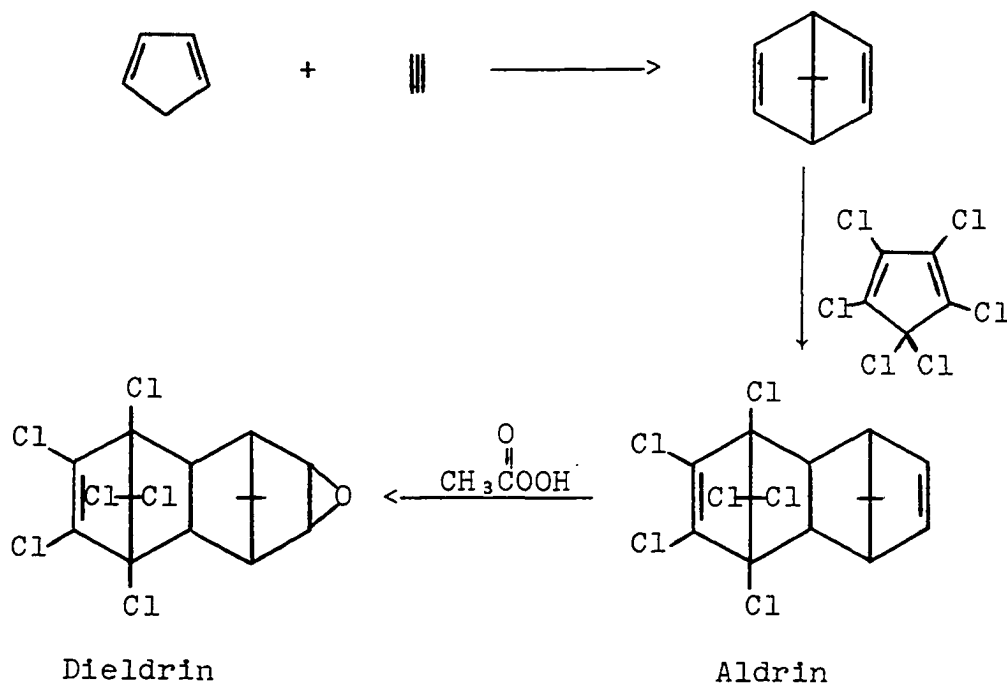
atomic coordinates for the endrin molecule are within two standard deviations of those determined in this laboratory.

THE CRYSTAL AND MOLECULAR STRUCTURE OF THE
INSECTICIDE DIELDRIN

Introduction

Dieldrin, a geometrical isomer of endrin, is perhaps the most widely used of the cyclodiene insecticides and the most widely publicized because of concern over environmental contamination by relatively stable residues in the soil.

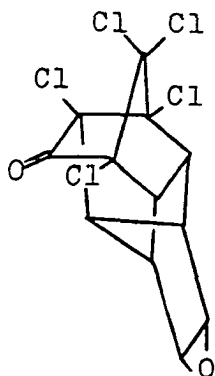
Dieldrin may be prepared by the Diels-Alder condensation reactions²⁹



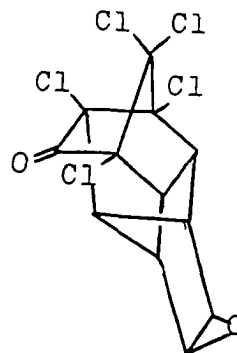
There are two different structural formulas in the literature, 1,2,3,4,10,10-hexachloro-6,7-epoxy-1,4,4a,5,6,7,8,8a-octahydro-endo-exo-1,4:5,8-dimethanonaphthalene^{30,32-34} and 1,2,3,4,10,10-hexachloro-6,7-epoxy-1,4,4a,5,6,7,8,8a-octahydro-exo-endo-1,4:5,8-dimethanonaphthalene,³⁵ the result, as with endrin, of a difference in American and British conventions in nomenclature. The orientation of the epoxide ring is not defined.

Aldrin is converted to dieldrin in the soil and in plant and animal tissues.³⁰ An X-ray crystallographic study of aldrin was completed by DeLacy and Kennard⁴¹ in 1972.

The major metabolites of dieldrin and aldrin were isolated from poisoned rats by Damico, Chen, Costello, and Haenni.⁴² The metabolites, two forms of Klein's metabolite, were postulated, on the basis of IR, Raman, and mass spectrometric evidence, to be the isomers I and II, varying



I



II

in the exo- or endo- orientation of the epoxide ring. The question has since been raised by Benson⁴³ of the possibility of the existence of two dieldrin structures, as aldrin is first converted to dieldrin in biological systems.

In this crystallographic study, we hoped to establish the position of the epoxide ring and to provide atomic coordinates in the molecule for accurate model building as an aid in the elucidation of structure-toxicity relationships.

Experimental

Crystals of analytical grade dieldrin, m.p. 175-176°, were obtained from P. A. Dahm. Microscopic examination revealed that the crystals were needle-shaped tetragonal prisms with sharply defined faces. The crystals were too fragile to seal in thin-walled glass capillaries and were therefore mounted on glass fibers. Preliminary precession photographs showed that it would be necessary to use a relatively large crystal for many diffraction maxima to be observed. The photographs exhibited mmm diffraction symmetry with systematic alternate extinctions along the three axes $h,0,0: h \neq 2n$, $0,k,0: k \neq 2n$, and $0,0,l: l \neq 2n$ uniquely defining the orthorhombic space group $P2_12_12_1$.

The unit cell parameters at 24° are $a=38.412(12)$, $b=14.124(4)$, and $c=8.098(3)\text{\AA}$. These parameters and their standard deviations were obtained by a least-squares fit to 14 independent reflection angles⁴ whose centers were determined by left-right, top-bottom beam splitting on a previously aligned Hilger-Watts diffractometer (Cu K α radiation, $\lambda=1.5418\text{\AA}$). Any error in the instrumental zero was eliminated by centering the reflection at both $+2\theta$ and -2θ . A calculated density of 1.729 g/cc for 12 molecules per unit cell agrees well with the observed density 1.75 g/cc.⁴⁴

The fact that dieldrin crystallizes with 12 molecules in the unit cell, three in the asymmetric unit, is rather unusual. Very often when a compound crystallizes with more than one or two formula units in the asymmetric unit there are structural differences between molecules. There existed, therefore, a slight possibility of there having been cocrystallization of more than one isomer, assuming a eutectic melting point. The large unit cell size also meant that the structure was a much more difficult crystallographic problem than endrin, with 57 instead of 19 non-hydrogen symmetry-unrelated atoms. Unless an exceedingly large amount of data could be collected, the data-parameter ratio would not be high enough to obtain meaningful least squares refinement and small standard deviations.

For data collection, a crystal with dimensions 0.16 x 0.18 x 0.40 mm was mounted on a glass fiber with the (120) axis coincident with the phi axis of the diffractometer. Intensity data were taken at room temperature (24°) using Ni-filtered Cu K α radiation ($\lambda = 1.5418\text{\AA}$) radiation on a fully automated Hilger-Watts four-circle diffractometer equipped with a scintillation counter and interfaced to an SDS-910 computer in a real-time mode. All data within a theta sphere of 55° were measured using a θ -2 θ stepscan technique. A counting rate of 0.4096 sec per step was used with a variable scan range of 50 steps of 0.01 degree in theta plus 2 steps per degree theta. Stationary-counter measurements of the background were made at the beginning and end of each scan, with each background measurement being made for one-half the total scan time. A total of 3258 intensities were measured. As a check on electronic and crystal stability, three standard reflections were measured periodically during data collection. These reflections decreased slowly in intensity, the total decrease being 22%, and the data were appropriately corrected.

The intensity data were also corrected for Lorentz-polarization effects and for absorption ($\mu = 108 \text{ cm}^{-1}$). The absorption correction was calculated using the Tompa-Alcock absorption correction program;^{36,37} the maximum

and minimum transmission factors were 0.30 and 0.013, respectively.

Standard deviations (σ_I) in the intensities were calculated by

$$(\sigma_I)^2 = [TC + BC + (0.05 \times TC)^2 + (0.05 \times BC)^2 + (0.05 \times NET)^2] / A^2$$

where TC, BC, NET, and A are the total count, background count, net count, and transmission factor, respectively. The quantities 0.05 represent estimates for non-statistical errors in the total count, background count, and absorption correction, respectively. Values for σ_F were obtained by the finite difference method.⁶ Of the 3258 measured intensities, the 2150 with $F_o > 2.5\sigma_F$ were considered observed and were used in the refinement.

Solution and Refinement

The structure was solved using direct methods with the MULTAN programs of Main, et al.³⁸ The 18 chlorine atoms, six in each of three molecules in the asymmetric unit, were located by an E-map based on 195 reflections with $E > 1.50$, with the phases determined by application of the tangent formula of Karle and Hauptman.³⁹

A structure factor calculation with refinement of the scale factor gave a conventional agreement factor ($R = \Sigma ||F_o| - |F_c|| / \Sigma |F_o|$) of 0.380. The remaining 39 light

atoms were located by a series of structure factor calculations and electron density maps, with six carbon atoms in particular, in one molecule, very difficult to distinguish in the final electron density maps.

The structure was refined by a full-matrix least-squares procedure using a local modification of Busing, Martin, and Levy's OR FLS.⁸ The function minimized was $\Sigma\omega(|F_o| - |F_c|)^2$ where ω is the weight defined as $1/\sigma^2(F_o)$. Isotropic refinement resulted in a conventional discrepancy factor of 0.192 and a weighted discrepancy factor ($\omega R = [\Sigma\omega(|F_o| - |F_c|)^2/\Sigma\omega|F_o|^2]^{1/2}$) of 0.198. The scattering factors for C, O, and Cl are from the tables by Hanson, Herman, Lea, and Skillman.¹¹

Although there appeared to be some problem with refinement of several carbon atoms in one molecule, refinement of the structure was continued with anisotropic temperature factors for chlorine atoms and isotropic temperature factors for the other atoms until convergence at $R=0.156$ and $\omega R=0.157$, with the average shift/error for the last cycle of 0.06. The data-parameter ratios for isotropic and partial anisotropic refinement were 9.4 and 6.7, respectively. A final electron density difference map showed no peaks greater than $1.0e^-/\text{\AA}^3$.

The final positional and thermal parameters for the chlorine atoms are listed in Tables 12 and 13, with the

Table 12. Final chlorine atom positional parameters
($\times 10^4$) for dieldrin

Atom	x	y	z
Cl(11)	76(3)	633(6)	8022(15)
Cl(12)	4510(3)	3922(7)	9078(21)
Cl(13)	805(3)	4011(9)	2544(24)
Cl(14)	406(3)	2238(7)	4478(17)
Cl(15)	4805(3)	1837(7)	2748(13)
Cl(16)	503(3)	3833(8)	7591(16)
Cl(21)	1750(3)	3484(6)	5356(16)
Cl(22)	2340(2)	2285(7)	7527(15)
Cl(23)	2362(2)	23(6)	6084(14)
Cl(24)	3233(2)	219(6)	8186(13)
Cl(25)	1334(2)	1951(8)	2622(14)
Cl(26)	2083(2)	2011(7)	2448(14)
Cl(31)	4119(2)	3928(9)	3955(22)
Cl(32)	3723(4)	2295(11)	6351(20)
Cl(33)	3007(2)	1563(6)	4517(16)
Cl(34)	2934(3)	2636(9)	836(14)
Cl(35)	3606(3)	4237(8)	357(15)
Cl(36)	3842(4)	2326(9)	1307(25)

Table 13. Final chlorine atom anisotropic thermal parameters ($\times 10^4$) for dieldrin^a

Atom	β_{11}	β_{22}	β_{33}	β_{12}	β_{13}	β_{23}
Cl(11)	13(1)	50(5)	324(31)	-2(2)	-11(6)	27(11)
Cl(12)	8(1)	68(7)	603(46)	-10(2)	0(7)	-13(16)
Cl(13)	4(1)	153(11)	683(52)	5(2)	13(7)	-39(26)
Cl(14)	13(1)	52(6)	363(31)	8(2)	-15(6)	-38(13)
Cl(15)	18(1)	78(7)	146(20)	3(3)	2(5)	22(11)
Cl(16)	15(1)	90(8)	288(28)	8(2)	-32(6)	-37(14)
Cl(21)	12(1)	43(5)	348(29)	3(2)	-5(5)	2(12)
Cl(22)	8(1)	90(7)	264(24)	-12(2)	-6(5)	-24(14)

^aThe B_{ij} are defined by: $T = \exp[-(h^2\beta_{11}+k^2\beta_{22}+l^2\beta_{33}+2hk\beta_{12}+2hl\beta_{13}+2kl\beta_{23})]$.

Table 13 (Continued)

Atom	β_{11}	β_{22}	β_{33}	β_{12}	β_{13}	β_{23}
C1(23)	6(1)	60(6)	314(26)	2(2)	-3(4)	34(12)
C1(24)	9(1)	58(5)	192(21)	-1(2)	-3(4)	11(10)
C1(25)	7(1)	107(8)	190(21)	9(2)	2(4)	39(13)
C1(26)	8(1)	79(7)	239(23)	-3(2)	8(4)	6(12)
C1(31)	5(1)	128(10)	622(50)	-7(2)	1(6)	1(20)
C1(32)	16(1)	133(11)	440(40)	-2(3)	-33(7)	90(20)
C1(33)	8(1)	50(6)	383(30)	0(2)	-5(5)	13(12)
C1(34)	12(1)	121(9)	186(23)	0(3)	-8(5)	-28(13)
C1(35)	18(1)	77(7)	247(26)	6(3)	17(6)	45(13)
C1(36)	18(2)	65(8)	796(63)	-3(3)	55(9)	-37(19)

final carbon and oxygen positional parameters and isotropic temperature factors listed in Table 14. The standard deviations were derived from the inverse matrix. In Table 15 are listed the observed and calculated structure factors. Interatomic distances and angles were calculated using OR FFE¹² and the variance-covariance matrix from the last least-squares cycle.

Supplementary Data and Refinement

The dieldrin structure did not refine well enough to give bond distances and angles of the accuracy usually expected from an X-ray crystallographic structure determination. The rather poor results could have been caused by one of several problems. In using direct methods, an incorrect phase set may have been chosen such that the first 18 atom positions were translated from their correct positions in the unit cell; we could find no evidence that this had happened. The dieldrin molecule is overall somewhat cylindrical in shape, and it may well be that the packing is such that one molecule can have some rotational disorder. It is not likely that poor data would preferentially affect the accurate determination of a part of one molecule, but due to the decomposition problem and large absorption correction using Cu K α radiation, the data set was suspect. Accordingly, we

Table 14. Final oxygen and carbon atom positional and thermal parameters for dieldrin^a

Atom	x	y	z	B
O(1)	4294(7)	682(18)	9428(36)	6.6(6)
O(2)	980(7)	572(18)	9455(37)	6.9(7)
O(3)	2259(10)	4420(25)	1186(49)	11.0(10)
C(101)	36(8)	4751(21)	5585(43)	4.0(7)
C(102)	355(10)	4939(28)	4640(52)	5.9(9)
C(103)	472(13)	4180(35)	3964(65)	8.1(13)
C(104)	234(10)	3396(29)	4471(56)	6.5(10)
C(105)	4854(9)	1564(22)	6295(42)	3.8(7)
C(106)	4862(9)	1329(23)	8231(45)	4.6(8)
C(107)	4444(9)	1410(23)	8361(46)	4.6(8)
C(108)	4333(9)	456(24)	7772(50)	5.0(8)
C(109)	4646(9)	-79(23)	7349(47)	5.6(9)
C(110)	4733(10)	560(27)	5670(52)	6.1(10)
C(111)	145(15)	3717(37)	6309(74)	11.1(16)
C(112)	4900(9)	314(24)	8486(47)	4.9(8)
C(201)	1749(8)	2232(21)	5581(44)	3.9(7)
C(202)	2074(10)	1812(27)	5992(51)	5.9(10)
C(203)	2081(9)	898(23)	5607(47)	4.5(8)
C(204)	1766(7)	752(17)	4594(37)	2.2(5)

^aThe positional parameters and their standard errors are $\times 10^4$.

Table 14 (Continued)

Atom	x	y	z	B
C(205)	1423(9)	765(25)	5721(51)	5.5(9)
C(206)	1415(9)	159(24)	7513(50)	5.5(8)
C(207)	1029(9)	306(23)	7866(51)	4.9(8)
C(208)	1009(9)	1369(24)	8360(47)	4.7(8)
C(209)	1408(8)	1697(21)	8152(40)	3.1(7)
C(210)	1410(8)	1809(21)	6208(40)	3.0(7)
C(211)	1728(10)	1776(26)	3762(51)	6.1(9)
C(212)	1600(8)	755(21)	8621(41)	4.1(8)
C(301)	3695(14)	3593(39)	3623(73)	9.7(15)
C(302)	3564(15)	2845(40)	4574(74)	10.7(15)
C(303)	3235(13)	2472(32)	3819(63)	8.5(12)
C(304)	3217(10)	3069(26)	2349(53)	6.3(9)
C(305)	3054(19)	4052(48)	3048(89)	14.4(21)
C(306)	2788(10)	4110(25)	4558(51)	5.3(9)
C(307)	2811(18)	5350(47)	4528(90)	13.5(20)
C(308)	1906(12)	4435(30)	485(60)	7.4(11)
C(309)	3309(15)	4674(39)	5858(71)	10.9(15)
C(310)	3411(13)	4391(34)	3758(65)	8.9(14)
C(311)	3609(11)	3333(30)	1924(58)	6.9(11)
C(312)	3004(10)	3984(25)	6054(49)	5.4(9)

decided to collect data on a second dieldrin crystal in an attempt to minimize these effects.

Data were collected on a new diffractometer designed and built in the Ames Laboratory. Peak height data were collected using MoK α radiation ($\mu=11.7 \text{ cm}^{-1}$) on a crystal of dimensions 0.12 x 0.17 x 0.38 mm at the rate of 100 reflections/hr by the method described by Johnson and Jacobson.⁴⁵ A total of 2413 intensity data were collected, with there being no observable decomposition of the crystal.

The structure was refined with the new intensity data (the 1454 data with $F_o > 3\sigma_F$) to final isotropic convergence at $R=0.118$ and $wR=0.132$. The data-parameter ratio for isotropic refinement was 6.4, which is low, and the average standard deviation in bond lengths was 0.05\AA .

As in the refinement of the structure with the first set of data, the atoms with the highest temperature factors (C301, C302, C305, C307, C308, C309, O3 and C136) were all in the third molecule. This tends to make us believe that there is some rotational disorder of the third molecule in the solid state, and that any further work on the dieldrin structure would be unproductive.

The atom positions, distances, and angles reported are those obtained from refinement of the structure with the first set of data.

Discussion

The three crystallographically unique dieldrin molecules have the same molecular structure. The dieldrin molecule is shown in Figure 6 where it can be seen that the epoxide ring is exo with respect to the non-chlorinated norbornene ring. The structural formula should be written 1,2,3,4,10,10-hexachloro-6,7-exo-epoxy-1,4,4a,5,6,7,8,8a-octahydro-endo-exo-1,4:5,8-dimethanonaphthalene.

Bond distances and angles for the three molecules in the asymmetric unit are given in Tables 16 and 17 and the bond distances are also presented in Figure 7 for comparison of the three molecules. The errors associated with the distances and angles are quite large, and extensive discussion is probably not worthwhile.

Within standard deviations, the molecule appears to be symmetric with respect to the non-crystallographic mirror plane which bisects the two methano bridges with the exception of the angles describing fusion of the two norbornene rings. These are C(104)-C(105)-C(106), C(209)-C(210)-C(201), C(309)-C(310)-C(301): 112(3), 112(3) and 112(4)^o on one side; and C(109)-C(110)-C(101), C(204)-C(205)-C(206), C(304)-C(305)-C(306): 120(3), 124(4), and 121(3)^o, respectively, on the other side of the "mirror". In the aldrin structure⁴¹ these two angles are both 122^o and the molecule does look more symmetrical.

Figure 6. View of the dieldrin molecule, 1,2,3,4,10,10-hexachloro-6,7-exo-epoxy-1,4,4a,5,6,7,8,8a-octahydro-endo-exo-1,4:5,8-dimethanonaphthalene

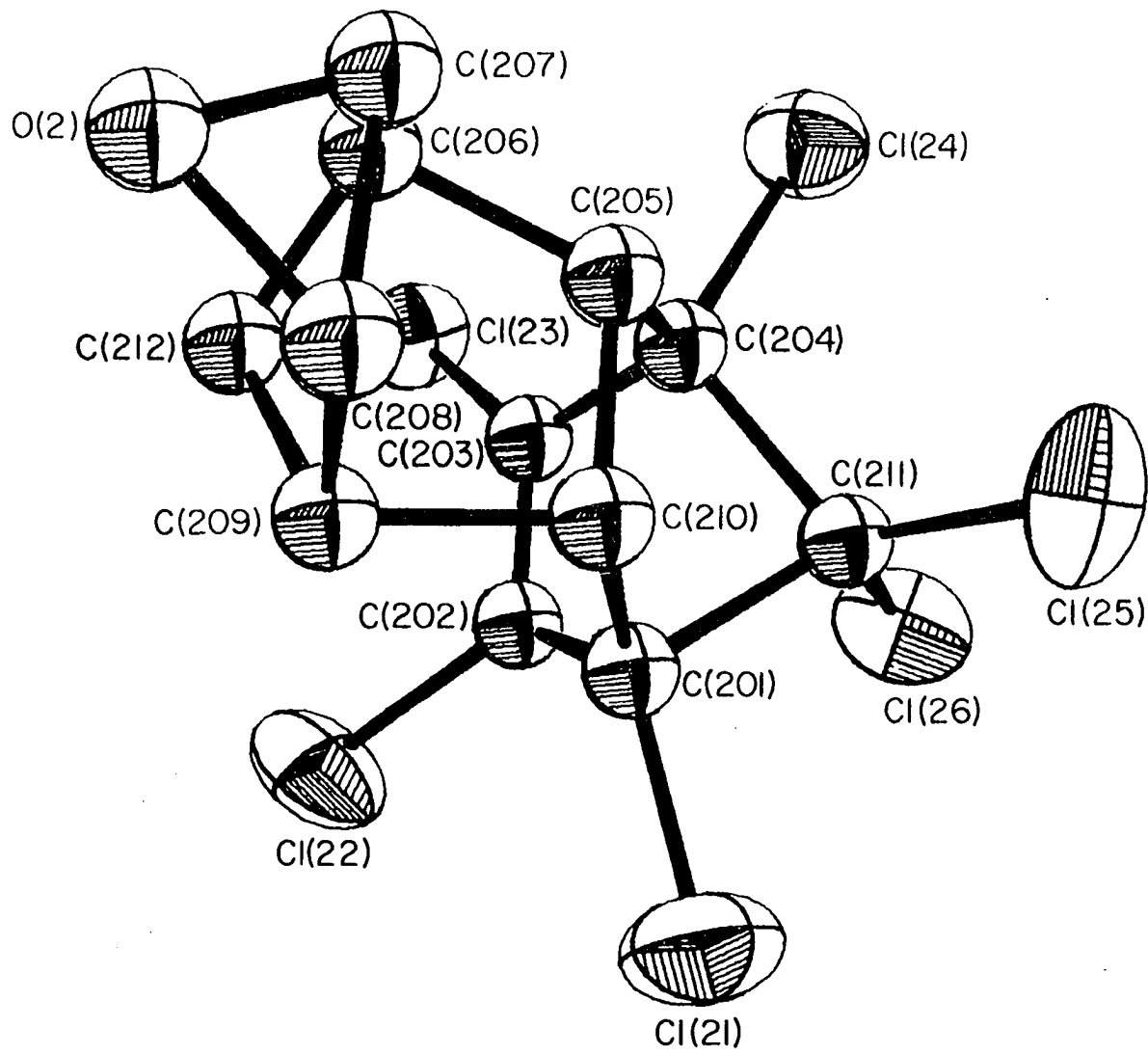


Table 16. Bond distances for dieldrin (\AA)

(a) Molecule 1

C(101)-C(102)	1.47(4)	C(111)-C(104)	1.59(6)
C(102)-C(103)	1.28(5)	C(111)-C(101)	1.63(5)
C(103)-C(104)	1.49(5)	C(112)-C(106)	1.46(4)
C(104)-C(105)	1.59(5)	C(112)-C(109)	1.45(4)
C(105)-C(106)	1.60(4)	C(107)-O(1)	1.46(4)
C(106)-C(107)	1.61(4)	C(108)-O(1)	1.38(4)
C(107)-C(108)	1.49(4)	C(101)-Cl(11)	1.73(3)
C(108)-C(109)	1.46(4)	C(102)-Cl(12)	1.75(4)
C(109)-C(110)	1.66(5)	C(103)-Cl(13)	1.74(5)
C(110)-C(101)	1.61(4)	C(104)-Cl(14)	1.76(4)
C(105)-C(110)	1.57(4)	C(111)-Cl(15)	1.71(5)
		C(111)-Cl(16)	1.73(5)

(b) Molecule 2

C(201)-C(202)	1.42(4)	C(211)-C(204)	1.60(4)
C(202)-C(203)	1.33(4)	C(211)-C(201)	1.61(5)
C(203)-C(204)	1.48(4)	C(212)-C(206)	1.42(4)
C(204)-C(205)	1.60(4)	C(212)-C(209)	1.57(4)
C(205)-C(206)	1.68(5)	C(207)-O(2)	1.35(4)
C(206)-C(207)	1.52(4)	C(208)-O(2)	1.43(4)

Table 16 (Continued)

(b) Molecule 2

C(207)-C(208)	1.56(4)	C(201)-Cl(21)	1.78(3)
C(208)-C(209)	1.61(4)	C(202)-Cl(22)	1.74(4)
C(209)-C(210)	1.58(4)	C(203)-Cl(23)	1.68(3)
C(210)-C(201)	1.52(4)	C(204)-Cl(24)	1.78(3)
C(205)-C(210)	1.53(4)	C(211)-Cl(25)	1.79(4)
		C(211)-Cl(26)	1.76(4)

(c) Molecule 3

C(301)-C(302)	1.40(6)	C(311)-C(304)	1.59(5)
C(302)-C(303)	1.50(6)	C(311)-C(301)	1.46(6)
C(303)-C(304)	1.46(5)	C(312)-C(306)	1.48(4)
C(304)-C(305)	1.62(7)	C(312)-C(309)	1.53(6)
C(305)-C(306)	1.60(7)	C(307)-O(3)	1.41(6)
C(306)-C(307)	1.75(7)	C(308)-O(3)	1.47(5)
C(307)-C(308)	1.37(7)	C(301)-Cl(31)	1.72(5)
C(308)-C(309)	1.53(6)	C(302)-Cl(32)	1.75(5)
C(309)-C(310)	1.79(7)	C(303)-Cl(33)	1.65(4)
C(310)-C(301)	1.57(6)	C(304)-Cl(34)	1.75(4)
C(305)-C(310)	1.57(7)	C(311)-Cl(35)	1.80(4)
		C(311)-Cl(36)	1.75(4)

Table 17. Bond angles for dieldrin (deg).

(a) Molecule 1

C(101)-C(102)-C(103)	111(4)	C(105)-C(104)-C(111)	99(3)
C(102)-C(103)-C(104)	107(4)	C(102)-C(101)-C(111)	98(3)
C(103)-C(104)-C(105)	115(3)	C(110)-C(101)-C(111)	100(3)
C(104)-C(105)-C(106)	112(3)	C(108)-C(107)-O(1)	56(2)
C(105)-C(106)-C(107)	92(3)	C(107)-C(108)-O(1)	61(2)
C(106)-C(107)-C(108)	102(2)	C(107)-O(1)-C(108)	63(2)
C(107)-C(108)-C(109)	108(3)	C1(11)-C(101)-C(110)	116(2)
C(109)-C(110)-C(101)	121(3)	C1(11)-C(101)-C(102)	114(2)
C(110)-C(101)-C(102)	109(3)	C1(12)-C(102)-C(101)	123(3)
C(104)-C(111)-C(101)	89(3)	C1(12)-C(102)-C(103)	124(3)
C(106)-C(112)-C(109)	103(3)	C1(13)-C(103)-C(102)	131(4)
C(104)-C(105)-C(110)	100(3)	C1(13)-C(103)-C(104)	122(3)
C(106)-C(105)-C(110)	98(3)	C1(14)-C(104)-C(103)	117(3)
C(101)-C(110)-C(105)	104(3)	C1(14)-C(104)-C(105)	112(2)
C(109)-C(110)-C(105)	107(3)	C1(14)-C(104)-C(111)	110(3)
C(110)-C(109)-C(112)	100(3)	C1(11)-C(101)-C(111)	118(3)
C(108)-C(109)-C(112)	102(3)	C1(15)-C(111)-C(104)	117(4)
C(105)-C(106)-C(112)	110(3)	C1(15)-C(111)-C(101)	112(3)
C(107)-C(106)-C(112)	99(3)	C1(16)-C(111)-C(104)	115(4)
C(103)-C(104)-C(111)	100(4)	C1(16)-C(111)-C(101)	110(3)

Table 17 (Continued)

(b) Molecule 2

C(201)-C(202)-C(203)	112(3)	C(205)-C(204)-C(211)	99(2)
C(202)-C(203)-C(204)	104(3)	C(202)-C(201)-C(211)	95(3)
C(203)-C(204)-C(205)	111(2)	C(210)-C(201)-C(211)	96(2)
C(204)-C(205)-C(206)	120(3)	C(208)-C(207)-O(2)	58(2)
C(205)-C(206)-C(207)	96(3)	C(207)-C(208)-O(2)	54(2)
C(206)-C(207)-C(208)	103(3)	C(207)-O(2)-C(208)	68(2)
C(207)-C(208)-C(209)	102(2)	C1(21)-C(201)-C(210)	115(2)
C(209)-C(210)-C(201)	112(3)	C1(21)-C(201)-C(202)	116(2)
C(210)-C(201)-C(202)	121(3)	C1(22)-C(202)-C(201)	121(3)
C(204)-C(211)-C(201)	89(2)	C1(22)-C(202)-C(203)	122(3)
C(206)-C(212)-C(209)	97(2)	C1(23)-C(203)-C(202)	132(3)
C(204)-C(205)-C(210)	101(2)	C1(23)-C(203)-C(204)	123(2)
C(206)-C(205)-C(210)	106(3)	C1(24)-C(204)-C(203)	117(2)
C(201)-C(210)-C(205)	106(2)	C1(24)-C(204)-C(205)	112(2)
C(209)-C(210)-C(205)	99(3)	C1(24)-C(204)-C(211)	115(2)
C(210)-C(209)-C(212)	109(3)	C1(21)-C(201)-C(211)	108(2)
C(208)-C(209)-C(212)	100(2)	C1(25)-C(211)-C(204)	115(2)
C(205)-C(206)-C(212)	103(2)	C1(25)-C(211)-C(201)	117(2)
C(207)-C(206)-C(212)	107(3)	C1(26)-C(211)-C(204)	111(2)
C(203)-C(204)-C(211)	100(2)	C1(26)-C(211)-C(201)	116(2)

Table 17 (Continued)

(c) Molecule 3

C(301)-C(302)-C(303)	110(5)	C(305)-C(304)-C(311)	104(3)
C(302)-C(303)-C(304)	100(4)	C(302)-C(301)-C(311)	104(4)
C(303)-C(304)-C(305)	103(4)	C(310)-C(301)-C(311)	95(4)
C(304)-C(305)-C(306)	124(4)	C(308)-C(307)-O(3)	64(4)
C(305)-C(306)-C(307)	90(4)	C(307)-C(308)-O(3)	59(3)
C(306)-C(307)-C(308)	105(4)	C(307)-O(3)-C(308)	57(3)
C(307)-C(308)-C(309)	111(4)	C1(31)-C(301)-C(310)	117(4)
C(309)-C(310)-C(301)	112(4)	C1(31)-C(301)-C(302)	118(4)
C(310)-C(301)-C(302)	105(4)	C1(32)-C(302)-C(301)	131(4)
C(304)-C(311)-C(301)	94(4)	C1(32)-C(302)-C(303)	118(4)
C(306)-C(312)-C(309)	105(3)	C1(33)-C(303)-C(302)	125(4)
C(304)-C(305)-C(310)	93(4)	C1(33)-C(303)-C(304)	135(4)
C(306)-C(305)-C(310)	105(4)	C1(34)-C(304)-C(303)	113(3)
C(301)-C(310)-C(305)	111(4)	C1(34)-C(304)-C(305)	107(3)
C(309)-C(310)-C(305)	103(4)	C1(34)-C(304)-C(311)	121(3)
C(310)-C(309)-C(312)	97(4)	C1(31)-C(301)-C(311)	115(4)
C(308)-C(309)-C(312)	98(4)	C1(35)-C(311)-C(304)	108(3)
C(305)-C(306)-C(312)	105(3)	C1(35)-C(311)-C(301)	119(3)
C(307)-C(306)-C(312)	96(3)	C1(36)-C(311)-C(304)	111(3)
C(303)-C(304)-C(311)	106(3)	C1(36)-C(311)-C(301)	111(4)

Figure 7. Bond distances (\AA) in the three crystallographically unique dieldrin molecules. The standard deviations in the bond lengths range from 0.04-0.07 \AA

Many of the bond angles in dieldrin deviate appreciably from trigonal or tetrahedral geometry, and is likely due to strain in the methano-bridged ring system. The average C-C single bond length is 1.57\AA , which is comparable to an average 1.56\AA in the endrin molecule.

The overall shape of the molecule is somewhat cylindrical with the five chlorine atoms Cl(1)-Cl(5) describing the maximum circumference of the cylinder. Dieldrin is more elongated than endrin, with the length of the molecule, from the epoxide oxygen to a bridgehead chlorine, Cl(26), 7.36\AA . The longest distance across the approximate mirror plane, Cl(21) to Cl(24), is 5.52\AA . The comparable distances in endrin are 6.78 and 5.47\AA , respectively.

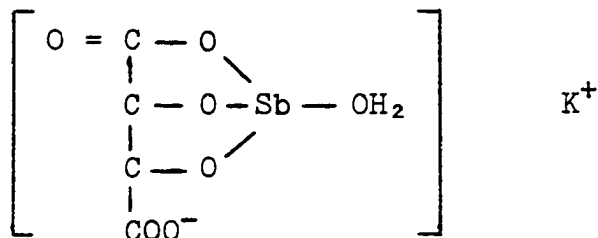
The distances between the midpoints of the C(202)-C(203) double bond and the C(207)-C(208) bond is 4.54\AA . In the aldrin molecule, this distance is 4.77\AA , and in endrin, 2.83\AA . If these two electronegative centers are important in the biological activity of these compounds, it may be significant that the two centers are much further apart in dieldrin and aldrin than in the endrin molecule.

X-RAY AND WHITE RADIATION NEUTRON DIFFRACTION STUDIES OF
OPTICALLY ACTIVE POTASSIUM ANTIMONY TARTRATE,
 $K_2Sb_2(\underline{d}\text{-}C_4H_2O_6)_2 \cdot 3H_2O$ (TARTAR EMETIC)

Introduction

Optically active potassium antimony tartrate, dipotassium di- μ -tartrato(4)-bis(antimonate(III)) trihydrate, is widely used in medicine for various parasitic diseases (as "tartar emetic"), as a mordant in dyeing, and to a limited extent, as an insecticide. Evidence for dimeric complex anions (tartrato(4)-bridged binuclear complexes) in this compound has recently been established on the basis of several X-ray structural investigations. These include the racemic salt, $K_2Sb_2(\underline{d}, \underline{l}\text{-}C_4H_2O_6)_2 \cdot 3H_2O$,⁴⁶ $(NH_4)_2Sb_2(\underline{d}\text{-}C_4H_2O_6)_2 \cdot 3H_2O$,⁴⁷ and an incomplete structural investigation of the optically active form, $K_2Sb_2(\underline{d}\text{-}C_4H_2O_6)_2 \cdot 3H_2O$.⁴⁸ In the latter study, the atom positions were located from electron density projections (from 690 film data) and with no refinement of atomic coordinates.

Previous to these studies several structural formulas had been advanced for optically active potassium antimony tartrate, the most widely accepted being the Reihlen and Hezel structure⁴⁹



A water molecule occupying a coordination site on the antimony atom was believed to ionize in solution, thus accounting for the acidic properties of tartar emetic solutions.

Because of our interest in the coordination geometry of antimony compounds, the elongation of X-Sb-X bonds trans to one another and lone pair effects, if any, we have completed a more accurate X-ray structural investigation on this compound incorporating a full-matrix least-squares refinement procedure. In addition, a neutron diffraction study using the white radiation neutron diffraction technique was undertaken to produce additional information on hydrogen atom positions and hydrogen bonding of the water molecules in the structure.

Experimental

Single crystals of $K_2Sb_2(\underline{d}\text{-C}_4\text{H}_2\text{O}_6)_2 \cdot 3\text{H}_2\text{O}$ were obtained by recrystallization of the commercially available compound from an aqueous solution. Preliminary Weissenberg and precession photographs exhibited mmm diffraction symmetry, indicating an orthorhombic space group. The systematic absences $hk\ell$ when $h + k \neq 2n$ and 00ℓ when $\ell \neq 2n$ uniquely determined the space group $C222_1$. The unit cell parameters at 25°C are $\underline{a} = 11.192(2)$, $\underline{b} = 11.696(3)$, and $\underline{c} = 25.932(5)\text{\AA}$, which agree well with those found by Kiosse, Golovastikov, and Belov.⁵⁰ The unit cell parameters and

their standard deviations were obtained by a least squares fit to 12 independent reflection angles whose centers were determined by left-right, top-bottom beam splitting on a previously aligned Hilger-Watts four-circle diffractometer (Cu K α radiation, $\lambda=1.5418\text{\AA}$). Any error in the instrumental zero was eliminated by centering the reflection at both $+2\theta$ and -2θ . The calculated density (2.606 g/cc) for eight dimers per unit cell agrees quite well with the observed density⁴⁴ of 2.607 g/cc.

In these studies preliminary to data collection there was a definite decomposition of the crystals which appeared to be due to loss of H₂O from the crystalline lattice. Freshly prepared crystals were clear with sharply defined faces; however, the faces became less sharply defined and coated with a white powder after 2-3 days exposure to X-rays or several days exposure to the atmosphere. A neutron activation analysis for oxygen content was performed in this laboratory. The results were consistent with three water molecules per dimer for freshly prepared crystals, but showed definite water loss on exposure to the atmosphere prior to analysis.

For data collection, a crystal with approximate dimensions 0.20 x 0.20 x 0.20 mm was mounted on a glass fiber with the c axis coincident with the spindle axis and well-coated with Duco cement glue to retard decomposition.

Intensity data were taken at room temperature (24°) using Zr-filtered Mo K α ($\lambda=0.71069\text{\AA}$) radiation on a fully-automated Hilger-Watts four-circle diffractometer equipped with a scintillation counter and interfaced to an SDS-910 computer in a real-time mode. 2779 Intensities were measured by counting at the peak center (θ_{hkl}) for ten seconds with two five second background counts at $\theta_{hkl} \pm (0.25 + (0.01 \times \theta_{hkl}))$. No dependence on chi or phi was observed. For conversion of peak height to integrated data, some integrated intensities were taken by the stepscan (moving crystal-moving counter) technique⁵ and a conversion table was prepared by plotting the integrated-peak height ratios as a function of theta.

As a general check on electronic and crystal stability, the intensities of three standard reflections were measured periodically during data collection. These reflections decreased slowly in intensity, the total decrease being 9%; such a decrease was felt to be quite acceptable and the data were appropriately corrected.

The intensity data were also corrected for Lorentz-polarization effects. The linear absorption coefficient, μ , is 38.8 cm^{-1} . Because of the nearly spherical shape of the crystal, the transmission factor was almost a constant, 0.46 - 0.47, so that an absorption correction was not considered necessary. Standard deviations (σ_I) in the

intensities were estimated from the total count (TC) and background count (BC) by

$$(\sigma_I)^2 = TC + BC + (0.05 \times TC)^2 + (0.05 \times BC)^2,$$

with the last two factors representing estimates for non-statistical errors in the total count and background count, respectively. Values for σ_F were obtained by the finite difference method.⁶ Of the 2779 reflections measured, the 2604 which had $F_o > 2.5\sigma_F$ were considered observed and were used in the refinement.

In order to obtain further information on the water molecule positions and on the hydrogen bonding in the solid state, neutron diffraction data were also collected.

Single crystals of $K_2Sb_2(\underline{d}\text{-C}_4\text{H}_2\text{O}_6)_2 \cdot 3\text{H}_2\text{O}$ were grown by slow evaporation from an aqueous solution. A small crystal of dimensions 2.3 x 1.9 x 1.2 mm was mounted with Duco cement on a thin vanadium rod. The crystal and rod were then encapsulated in a quartz capillary, with a small piece of wetted tissue at the end of the capillary to inhibit decomposition of the crystal by loss of H_2O . The crystal was aligned with (110) coincident with the spindle axis by precession techniques using Mo $K\alpha$ radiation.

Neutron diffraction data were taken using the white radiation neutron diffraction technique developed in this laboratory. The experimental arrangement at the 5 M.W.

Ames Laboratory Research Reactor is described elsewhere.^{51,52} The intensity data were taken on a previously aligned four-circle E. and A. diffractometer interfaced to a DATEX controller and to the same SDS-910 computer as used for collection of X-ray data. The orientation of the crystal was determined by using top/bottom left/right beam splitters to tune on three reflections with 2θ fixed.

The intensities were measured at points along Laue streaks at theta values calculated from the Bragg equation $n\lambda = 2d\sin\theta$ in increments of $\hat{\lambda} = 0.65\text{\AA}$ with $\hat{\lambda}$ initialized at 1.3\AA . (The maximum in the effective flux occurs near 1.3\AA .) Data for one octant were collected in the range $\theta = 7.50^\circ$ to $\theta = 45^\circ$. The counting period for each intensity was set by 8×10^5 monitor counts of the incident beam as detected by a U^{235} fission counter. As a check on crystal, flux, and electronic stability, the intensities of three standard reflections were measured between every 20 streaks, with the maximum deviation in any standard found to be only 2%. A total of 1766 intensities were measured along 1047 Laue streaks.

Background counts for the same counting period as the intensity data were taken on each side of the Laue streak at omega offsets of $\pm 0.75^\circ$ for the first 200 data points. A smooth curve was obtained for the background (the sum of the two background measurements) as a function of 2θ . The

observed intensity (I_o) was then calculated from the peak height (PH) and the background curve (BG) by

$$I_o = PH - 0.5(BG),$$

and the standard deviation (σ_I) in the intensity was calculated by

$$\sigma_I^2 = PH + 0.25(BG) + (0.02(I_o))^2.$$

The linear attenuation coefficient was calculated from hydrogen incoherent scattering and true absorption⁵³ by

$$\mu(\lambda) = (0.894 + 0.025(\frac{\lambda}{1.08\text{\AA}} - 1))\text{cm}^{-1},$$

which is adequate for the wavelength range 0.7 \AA to 3.0 \AA .

The transmission factor may be calculated from the expansion about λ_o

$$T(\lambda) = T(\lambda_o) + \frac{\partial T}{\partial \lambda} \Big|_{\lambda_o} (\lambda - \lambda_o) + \frac{1}{2} \frac{\partial^2 T}{\partial \lambda^2} \Big|_{\lambda_o} (\lambda - \lambda_o)^2 \dots$$

The maximum and minimum transmission factors at λ_o ($\lambda_o = 1.08\text{\AA}$) are 90% and 81%, respectively. The effect of higher order terms, evaluated for transmission at other wavelengths, has been shown by Hubbard, Quicksall and Jacobson⁵² to be relatively small.

Due to the small size of the crystal, a large percentage of intensity data were essentially at background level. Of the 1766 measured intensities, there were only $300 > 3\sigma_I$. Although few in number, we felt they would be sufficient for computation of a Fourier map and for locating the

hydrogen atoms and the orientation of hydrogen O-H bonds.

Solution and Refinement

In order to have an independent comparison with the work of Hsiang-Ch'i Mu,⁴⁸ the antimony atom positions were determined from an unsharpened Patterson map, and the other atom positions from subsequent structure factor calculations and electron density maps. All atoms are in general positions with the exception of the potassium atoms, eight of which occupy general positions and eight occupy two fourfold sets on the twofold axes. In the electron density maps one of the three H₂O oxygen atom peaks was of comparable size with the other oxygen peaks in the map, while the other two were barely distinguishable above background. The positional coordinates of these second two H₂O oxygen atom positions differed from the coordinates reported by Hsiang-Ch'i Mu, with there being no observable residual electron density at the Hsiang-Ch'i Mu positions even after later refinement of the structure.

The structure was refined by a full-matrix least-squares procedure using a local modification of Busing, Martin, and Levy's OR FLS⁸ with isotropic temperature factors to a conventional discrepancy factor ($R = \frac{\sum ||F_o| - |F_c||}{\sum |F_o|}$) of 0.139 and a weighted discrepancy factor

($\omega R = [\Sigma\omega(|F_o| - |F_c|)^2 / \Sigma\omega|F_o|^2]^{1/2}$) of 0.187. The function minimized was $\Sigma\omega(|F_o| - |F_c|)^2$ where ω is the weight defined as $1/\sigma^2(F_o)$. The scattering factors for Sb, O, C, and K^+ are from the tables by Doyle and Turner.⁹ The antimony and potassium scattering factors were modified by the real and imaginary parts of anomalous scattering¹⁰ and refinement was continued with anisotropic temperature factors. The two H₂O oxygen atoms which were low peaks in the electron density map were refined at half occupancy with isotropic temperature factors of 4.80 and 5.25. We interpret "half-occupancy" not as disorder, but rather that time-averaged over the period of the experiment half of these molecules were lost from the crystal.

The observed intensities by white radiation neutron diffraction are given by

$$I^{obs}(\theta) = k\Sigma\phi_{eff}(\lambda_n)T(\lambda_n)y(\lambda_n)[F_{nh}/d_{nh}^*]^2$$

where k is the scale factor, ϕ_{eff} is the effective flux, T is a transmission factor, y is an extinction correction, F_{nh} is the structure factor, and $\lambda_n = 2d_{nh}\sin\theta$.⁵¹

Approximate structure factors were obtained by the linear programming technique discussed by Hubbard, Quicksall, and Jacobson.⁵² Values for the scale factor k and flux parameters $P1$ (Maxwellian constant) and $P2$ (absorption constant) were 500, 2.55, and 0.30, respectively. The derived F 's were assigned phases of

structure factors calculated by using neutron scattering factors⁵⁴ and the heavy atom positional coordinates and anisotropic temperature factors from the X-ray determination. A scale factor was refined and a conventional agreement factor ($R = \Sigma ||F_o| - |F_c|| / \Sigma |F_o|$) of 0.45 was obtained.

A Fourier calculation (with grid resolution 0.17 x 0.18 x 0.20Å) clearly revealed the tartrate hydrogen positions, hydrogen atoms of one water molecule, with the hydrogen atoms of the other two water molecules (which had been refined at partial occupancy in the X-ray study) less clearly defined. Because of the large parameter to data ratio and because of the partial occupancy of some of the water molecules, full-matrix least-squares refinement using the neutron data did not appear worthwhile. Previous experience has shown that hydrogen atom positions taken from a Fourier map average within 0.17Å of their correct least-squares positions. The hydrogen atom positions estimated from the Fourier map are listed in Table 18.

Several least squares cycles were run, however, not varying the atom positions in the initial model to refine the flux and scale factors. Weighted agreement factors of the form

$$R_{I\omega} = \left\{ \frac{\sum_i \omega_i (I_i^{\text{obs}} - I_i^{\text{calc}})^2}{\sum_i \omega_i (I_i^{\text{obs}})^2} \right\}^{1/2}$$

Table 18. Approximate hydrogen atom positions determined by white radiation neutron diffraction for $K_2Sb_2(\underline{d}\text{-C}_4\text{H}_2\text{O}_6)_2 \cdot 3\text{H}_2\text{O}^a$

Atom	x	y	z
H(2)	0.4516	0.4375	0.1758
H(3)	0.3812	0.3359	0.2320
H(12)	0.1562	0.1359	0.0125
H(13)	0.0188	0.1172	0.0727
H(W1a)	0.3750	-0.2359	0.0820
H(W1b)	0.2516	-0.1875	0.0758
H(W2a)	0.3672	-0.2391	0.1578
H(W2b)	0.2453	-0.2641	0.2016
H(W3a)	0.3562	-0.0359	0.1500
H(W3b)	0.4531	0.0531	0.1500

^aThe hydrogen atoms are labeled according to the C atom to which they are bonded. For example, H(2) is bonded to C(2).

where $\omega_i = 1/\sigma_i^2$ were $R = 0.192$ for $I_{\text{obs}} > 3\sigma_I$ (300 intensities) and $R = 0.234$ for all data (1766 intensities) with final scale and flux parameters $k = 7.86$, $P1 = 2.50$, and $P2 = 0.56$. A listing of observed and calculated intensities is given in Table 19.

Refinement of the original structure with X-ray data was continued with addition of the hydrogen atom positions with X-ray scattering factors.¹¹ Convergence was reached at $R = 0.078$ and $\omega R = 0.100$ with the average shift/error for the last cycle of 0.01. In a final electron density difference map, all peaks above $1.0e^-/\text{\AA}^3$ (which ranged up to $3.4e^-/\text{\AA}^3$) lay in concentric spheres about the antimony atoms and were probably due to termination effects in the Fourier series.

Least squares refinement of the enantiomorph $((x,y,z) \rightarrow (-x,-y,-z))$ yielded higher agreement factors, $R = 0.080$ and $\omega R = 0.102$, which indicates that the absolute configuration is that of the d-tartaric acid dimer.

The observed and calculated structure factors are given in Table 20. The final positional and thermal parameters and standard deviations of the heavy atoms as derived from the inverse matrix of the final least squares cycle are given in Tables 21 and 22. Interatomic distances and their deviations were calculated using OR FFE and the variance-covariance matrix from the last least squares cycle.

Table 20. Observed and calculated structure factors (in electrons x10) for K₂Sb₂(d-C₄H₂O₆)₂·3H₂O

Table with multiple columns containing numerical data for observed and calculated structure factors. The table is organized into several sections, likely corresponding to different hkl reflections, with columns for observed values, calculated values, and their differences. The data is presented in a dense grid format.

Table 21. Final heavy atom positional parameters ($\times 10^4$)
for $\text{K}_2\text{Sb}_2(\underline{\text{d}}\text{-C}_4\text{H}_2\text{O}_6)_2 \cdot 3\text{H}_2\text{O}$

Atom	x	y	z
Sb(1)	3788(1)	3369(1)	487(0)
Sb(2)	1272(1)	1790(1)	1955(0)
K(1)	3664(4)	0	0
K(2)	0	5784(5)	2500
K(3)	3464(4)	634(4)	3938(2)
O(1)	4989(9)	2496(8)	988(4)
O(2)	3396(10)	4083(9)	1165(4)
O(3)	5679(9)	2420(10)	1791(5)
O(4)	3024(10)	2156(10)	1943(5)
O(5)	1221(11)	3585(13)	2059(5)
O(6)	2393(13)	5086(14)	2180(7)
O(11)	1969(10)	3938(9)	339(5)
O(12)	2879(9)	1926(8)	528(4)
O(13)	134(13)	3277(11)	162(7)
O(14)	794(12)	2232(12)	1244(5)
O(15)	1855(13)	3075(11)	1491(5)
O(16)	1689(14)	-407(10)	714(5)

Table 21 (Continued)

Atom	x	y	z
C(1)	5011(12)	2816(11)	1452(5)
C(2)	4103(13)	3768(12)	1583(5)
C(3)	3312(13)	3283(11)	2039(4)
C(4)	2275(16)	4090(15)	2095(6)
C(11)	1237(16)	3148(12)	286(6)
C(12)	1624(12)	1924(11)	396(5)
C(13)	912(12)	1433(14)	853(8)
C(14)	1561(15)	349(13)	1031(10)
O(W1)	2948(12)	-2563(14)	747(7)
O(W2)	3291(31)	-2421(29)	1854(12)
O(W3)	4441(30)	-191(32)	1393(12)

Table 22. Final heavy atom thermal parameters ($\times 10^4$) for $K_2Sb_2(d-C_4H_2O_6)_2 \cdot 3H_2O^a$

Atom	β_{11}	β_{22}	β_{33}	β_{12}	β_{13}	β_{23}
Sb(1)	47(1)	27(0)	8(0)	1(1)	3(0)	2(0)
Sb(2)	54(1)	72(1)	14(0)	-13(1)	14(0)	-2(1)
K(1)	44(3)	42(3)	26(1)	0	0	-12(1)
K(2)	64(4)	56(4)	18(1)	0	12(2)	0
K(3)	77(3)	56(3)	22(1)	-30(3)	1(1)	8(1)
O(1)	29(6)	43(6)	15(2)	7(6)	3(3)	2(3)
O(2)	50(8)	39(7)	12(2)	24(6)	-5(3)	-4(2)
O(3)	31(7)	60(8)	16(2)	8(6)	-6(3)	-5(3)
O(4)	39(7)	48(7)	16(2)	-1(6)	11(3)	0(3)
O(5)	59(9)	90(11)	18(2)	16(10)	6(4)	-8(4)
O(6)	75(11)	67(10)	28(3)	18(10)	8(5)	-12(5)
O(11)	61(9)	30(6)	17(2)	19(7)	-7(4)	2(3)

^aThe B_{ij} are defined by: $T = \exp[-(h^2\beta_{11} + k^2\beta_{22} + l^2\beta_{33} + 2hk\beta_{12} + 2hl\beta_{13} + 2kl\beta_{23})]$.
 For O(W2) and O(W3), only the isotropic temperature factors ($\times 10^4$) are given
 (under β_{11}).

Table 22 (Continued)

Atom	β_{11}	β_{22}	β_{33}	β_{12}	β_{13}	β_{23}
O(12)	41(7)	28(5)	12(1)	4(5)	-2(3)	4(2)
O(13)	95(13)	62(10)	33(4)	29(11)	-34(6)	-9(5)
O(14)	68(10)	66(10)	16(2)	7(8)	9(4)	5(4)
O(15)	93(12)	71(10)	12(2)	-22(10)	2(4)	8(4)
O(16)	98(13)	41(8)	17(2)	-10(8)	1(4)	-5(3)
C(1)	33(8)	32(8)	11(2)	-1(7)	4(3)	1(3)
C(2)	41(9)	36(8)	11(2)	-12(7)	3(3)	4(3)
C(3)	57(10)	37(8)	6(1)	27(8)	2(3)	2(3)
C(4)	61(13)	69(13)	9(2)	16(10)	5(4)	-3(4)
C(11)	76(14)	37(9)	14(2)	27(11)	-16(5)	-5(3)
C(12)	44(9)	33(8)	8(2)	19(7)	0(3)	-1(3)
C(13)	24(9)	51(11)	23(3)	-4(8)	5(4)	6(5)
C(14)	43(11)	33(10)	30(5)	-13(8)	8(6)	-3(5)
O(W1)	53(10)	79(12)	28(3)	9(9)	10(5)	6(5)
O(W2)	4.8(6)					
O(W3)	5.3(6)					

Discussion

In the unit cell of $K_2Sb_2(\underline{d}\text{-C}_4\text{H}_2\text{O}_6)_2 \cdot 3\text{H}_2\text{O}$ (Figure 8) are eight antimony-tartrate dimers. The dimers are tartrato-(4)-bridged binuclear complexes in which the two antimony atoms are each coordinated to a carboxyl oxygen atom and an α -hydroxyl atom from two tartrate groups. Racemic potassium antimony tartrate, $K_2Sb_2(\underline{d},\underline{l}\text{-C}_4\text{H}_2\text{O}_6)_2 \cdot 3\text{H}_2\text{O}$ crystallizes in space group $Pca2_1$ and contains a mixture of $Sb_2(\underline{d}\text{-C}_4\text{H}_2\text{O}_6)_2^{-2}$ and $Sb_2(\underline{l}\text{-C}_4\text{H}_2\text{O}_6)_2^{-2}$ isomers, two dd and two ll groups per unit cell.⁴⁶ In a review of tartrate complexes, Tapscott, Belford and Paul⁵⁵ have shown that a dl dimer is unstable with respect to dd and ll dimers because of steric effects.

The tartrato-(4)-bridged binuclear complex is shown in Figures 9 and 10, where it can be seen that the complex possesses approximate D_2 point symmetry. The tartrate quadridentate ligands form four five-membered nearly planar rings with the two antimony atoms, with dihedral angles between tartrate ligands at the antimony atoms of 99° . The least squares planes are given in Table 23.

Bond distances and angles in the antimony-tartrate dimer are given in Table 24. In general, these form a very consistent set of distances and angles related by the three non-crystallographic twofold rotation axes. The carboxylic acid carbon-oxygen bond distances where oxygen is also

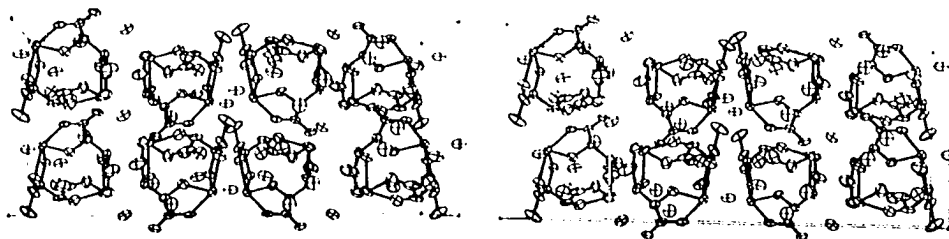


Figure 8. A stereo view of the $K_2Sb_2(\underline{d}\text{-C}_4\text{H}_2\text{O}_6)_2 \cdot 3\text{H}_2\text{O}$ unit cell. It is viewed looking down the b axis with a up and c across the page

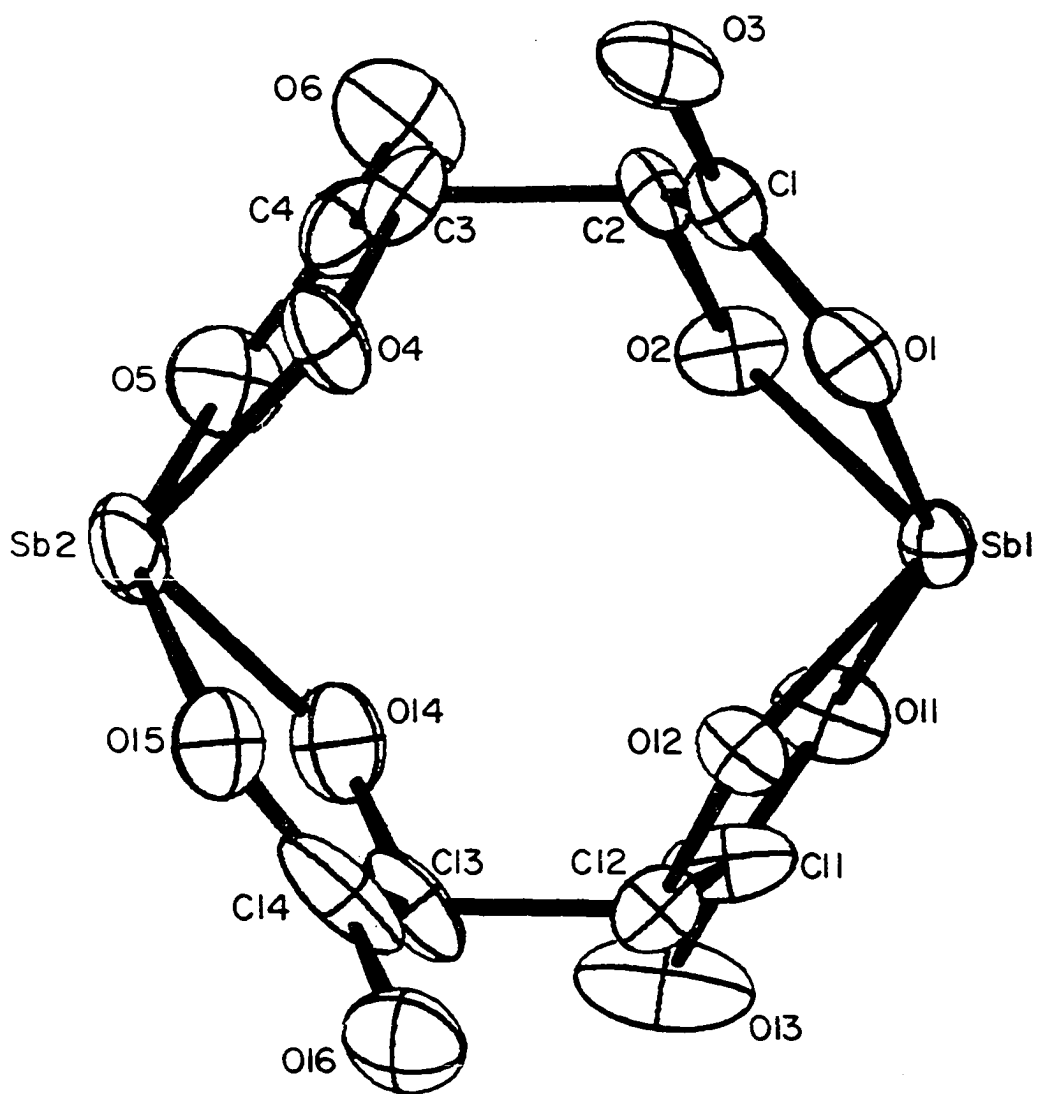


Figure 9. The $\text{Sb}_2(\underline{d}\text{-C}_4\text{H}_2\text{O}_6)_2^{-2}$ anion in optically active potassium antimony tartrate

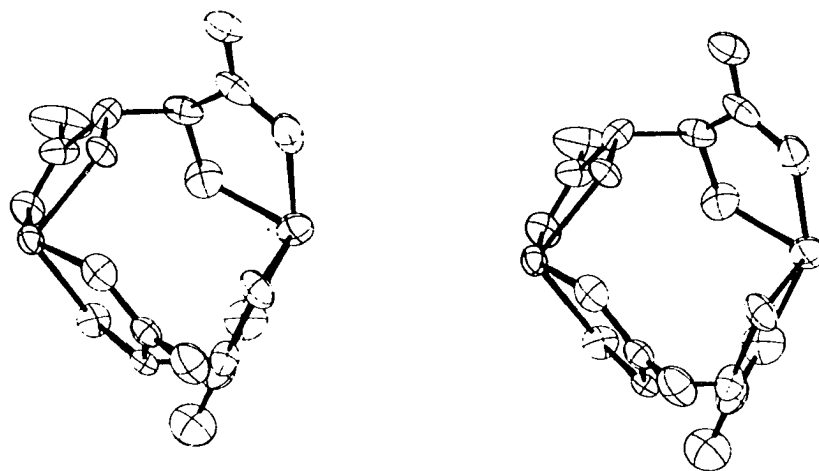


Figure 10. A stereo view of the antimony-tartrate dimer

Table 23. Least squares planes for $K_2Sb_2(\underline{d}\text{-C}_4\text{H}_2\text{O}_6)_2 \cdot 3\text{H}_2\text{O}^a$

(i) Sb(1), O(2), C(2), C(1), O(1)

Atom	Dev. (\AA)
Sb(1)	0.029
O(2)	-0.038
C(2)	0.028
C(1)	0.010
O(1)	-0.028

Equation:

$$0.6843x + 0.7010y - 0.2008z - 5.380 = 0$$

(ii) Sb(1), O(12), C(12), C(11), O(11)

Atom	Dev. (\AA)
Sb(1)	-0.043
O(12)	0.047
C(12)	-0.020
C(11)	-0.037
O(11)	0.054

Equation:

$$-0.1912x + 0.1239y + 0.9737z - 0.951 = 0$$

^aThe plane coordinates are defined relative to three orthogonal unit vectors along the a, b, and c directions.

Table 23 (Continued).

(iii) Sb(2), O(15), C(14), C(13), O(14)

Atom	Dev. (Å)
Sb(2)	-0.037
O(15)	0.035
C(14)	-0.013
C(13)	-0.036
O(14)	0.051

Equation:

$$0.8871x + 0.4220y - 0.1870z - 1.235 = 0$$

(iv) Sb(2), O(5), C(4), C(3), O(4)

Atom	Dev. (Å)
Sb(2)	0.024
O(5)	-0.022
C(4)	0.007
C(3)	0.024
O(4)	-0.033

Equation:

$$0.0195x - 0.1485y + 0.9887z - 4.705 = 0$$

Table 24. Bond distances and angles in the antimony-tartrate dimer

(a) Distances (Å)

Sb(1)-O(1)	2.13(1)	Sb(2)-O(5)	2.12(1)
Sb(1)-O(11)	2.18(1)	Sb(2)-O(15)	2.21(1)
Sb(1)-O(12)	1.97(1)	Sb(2)-O(14)	1.99(1)
Sb(1)-O(2)	2.00(1)	Sb(2)-O(4)	2.01(1)
C(1)-O(1)	1.26(2)	C(11)-O(11)	1.24(2)
C(1)-O(3)	1.24(2)	C(11)-O(13)	1.28(2)
C(1)-C(2)	1.55(2)	C(11)-C(12)	1.52(2)
C(2)-O(2)	1.39(2)	C(12)-O(12)	1.45(2)
C(2)-C(3)	1.58(2)	C(12)-C(13)	1.54(2)
C(3)-O(4)	1.38(2)	C(13)-O(14)	1.38(2)
C(3)-C(4)	1.50(2)	C(13)-C(14)	1.53(2)
C(4)-O(6)	1.19(2)	C(14)-O(16)	1.22(2)
C(4)-O(5)	1.32(2)	C(14)-O(15)	1.24(3)
C(2)-H(2)	0.96	C(12)-H(12)	0.97
C(3)-H(3)	0.92	C(13)-H(13)	0.93

Table 24 (Continued)

(b) Angles (deg)

O(1)-Sb(1)-O(11)	147.7(4)	O(5)-Sb(2)-O(15)	148.8(5)
O(2)-Sb(1)-O(12)	101.4(4)	O(4)-Sb(2)-O(14)	101.1(5)
O(11)-Sb(1)-O(12)	77.8(4)	O(15)-Sb(2)-O(14)	77.2(5)
O(1)-Sb(1)-O(2)	78.6(4)	O(5)-Sb(2)-O(4)	79.4(5)
Sb(1)-O(1)-C(1)	116.9(8)	Sb(1)-O(11)-C(11)	114.1(9)
O(1)-C(1)-O(3)	125.2(13)	O(11)-C(11)-O(13)	125.0(13)
O(3)-C(1)-C(2)	120.5(12)	O(13)-C(11)-C(12)	115.5(15)
O(1)-C(1)-C(2)	114.3(12)	O(11)-C(11)-C(12)	119.4(13)
C(1)-C(2)-O(2)	113.2(12)	C(11)-C(12)-O(12)	108.6(12)
C(2)-O(2)-Sb(1)	116.7(8)	C(12)-O(12)-Sb(1)	119.3(7)
O(2)-C(2)-C(3)	111.0(11)	O(12)-C(12)-C(13)	108.7(11)
C(2)-C(3)-O(4)	109.8(10)	C(12)-C(13)-O(14)	111.2(13)
C(3)-O(4)-Sb(2)	115.4(9)	C(13)-O(14)-Sb(2)	118.5(11)
O(4)-C(3)-C(4)	115.9(13)	O(14)-C(13)-C(14)	112.6(17)
C(3)-C(4)-O(6)	123.1(17)	C(13)-C(14)-O(16)	117.1(21)
C(3)-C(4)-O(5)	113.7(14)	C(13)-C(14)-O(15)	116.6(17)
O(6)-C(4)-O(5)	123.2(16)	O(16)-C(14)-O(15)	126.2(18)
C(4)-O(5)-Sb(2)	115.3(10)	C(14)-O(15)-Sb(2)	114.5(12)

bonded to antimony average $1.26(2)\text{\AA}$ compared to $1.23(2)\text{\AA}$ for carbon-uncoordinated oxygen atoms. The average C-C single bond distance is $1.54(2)\text{\AA}$.

The coordination of the two d-tartaric acid groups to the antimony atoms could be described in terms of either a distortion of a trigonal bipyramidal or a square planar bonding configuration. The axial bond angles (for two symmetry independent Sb atoms) O(1)-Sb(1)-O(11) and O(5)-Sb(2)-O(15) are 148° and 149° , and the equatorial bond angles O(2)-Sb(1)-O(12) and O(4)-Sb(2)-O(14) are 101° and 101° , respectively. Some distortion would, of course, be expected for coordination to a quadridentate ligand. Note, however, that the axial bonds are antimony-carboxyl oxygen bonds and the equatorial bonds are antimony-hydroxyl oxygen bonds. Antimony-carboxyl oxygen bond distances are 2.13, 2.18, 2.12, and 2.21\AA and antimony-hydroxyl oxygen bond distances are 1.97, 2.00, 1.99, and 2.01\AA . This correlates well with electron diffraction studies of PF_3Cl_2 ,⁵⁶ CH_3PF_4 , and $(\text{CH}_3)_2\text{PF}_3$,⁵⁷ for example, in which there is bond lengthening in the axial direction and in which the more electronegative substituents (fluorine atoms) are in axial positions. Bond lengthening in the axial direction, an average 0.17\AA in the potassium antimony tartrate structure, also correlates well with an average 0.24\AA lengthening of the antimony-halide bond in the axial direction in

antimony halide structures determined in this laboratory.⁵⁸ In such molecules the best bonding description is to neglect d-orbitals in the first approximation and use primarily p-orbitals for bonding, the longer bonds being three-center four-electron bonds.⁵⁷

Between tartrato-(4)-bridged binuclear anions there appear to be some electrostatic interaction with two antimony-oxygen interatomic distances shorter than the sum of the van der Waal radii, 3.60Å.⁵⁹ These are Sb(1)-O(13ⁱⁱ) and Sb(2)-O(6^{vi}), 2.97 and 3.35Å, respectively. These interactions are probably important only in the solid state.

Water molecules very often play a very important role in crystalline inorganic hydrated salts as ligands for metal ions and to minimize repulsion between anions.⁶⁰ The three water molecules in the potassium antimony tartrate structure are hydrogen bonded to one another as O(W1)-O(W2)-O(W3) chains, and are hydrogen bonded to tartrate oxygen atoms in different antimony tartrate dimers related by the c-centering operation (Figure 11). These hydrogen bonds, O(W1)-H(W1a)···O(13)(1/2 + x, -1/2 + y, z), O(W1)-H(W1b)···O(16), O(W2)-H(W2b)···O(3)(-1/2 + x, -1/2 + y, z), O(W3)-H(W3a)···O(15), connect the antimony tartrate dimers in infinite sheets parallel to the a-b plane, as seen in Figure 12. The hydrogen bonding distances and angles are given in Table 25.

Figure 11. View displaying the hydrogen-bonding of water molecules between antimony-tartrate dimers

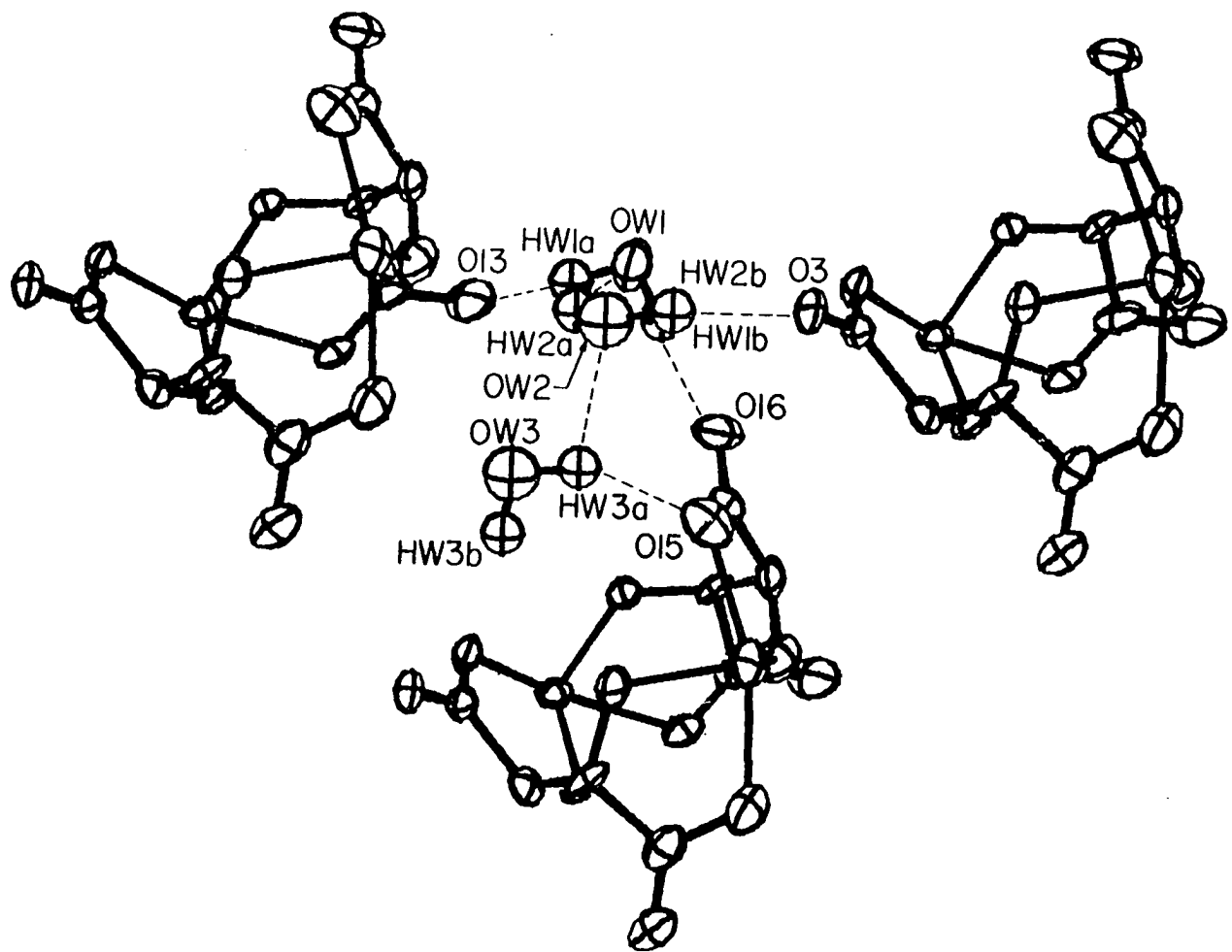


Figure 12. Intermolecular packing diagram showing the hydrogen-bonding network. This is a projection onto the a-b plane of four quarter-unit cell contents with $0 \leq z \leq 0.25$. There are four hydrogen-bonded infinite sheets for $0 \leq z \leq 1.0$

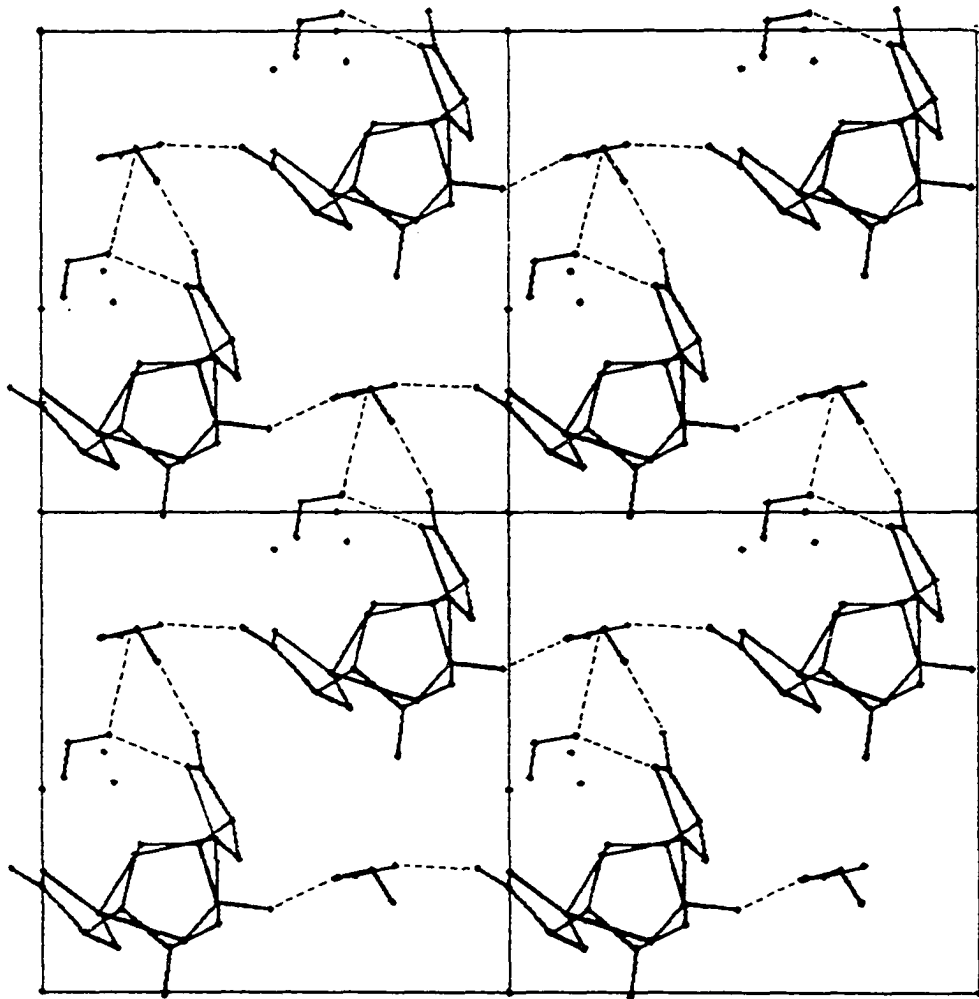


Table 25. Interatomic distances and angles involving water molecules^a

(a) Selected distances (Å) and angles (deg)

O(W1)-H(W1a)	0.95
O(W1)-H(W1b)	0.94
O(W2)-H(W2a)	0.83
O(W2)-H(W2b)	1.06
O(W3)-H(W3a)	1.04
O(W3)-H(W3b)	0.90
H(W1a)-O(W1)-H(W1b)	105
H(W2a)-O(W2)-H(W2b)	143
H(W3a)-O(W3)-H(W3b)	102
O(W1)-O(16)	2.89(2)
O(W1)-O(W2)	2.90(4)
O(W1)-O(13 ^{vii}) ^b	3.04(2)
O(W1)-K(3 ^{vi})	2.76(2)

^aThe hydrogen atom positions are estimated from the neutron Fourier synthesis.

^bThe superscripts used in this table and in the text refer to the following transformations:

i	x	-y	-z	vivi	$\frac{1}{2}-x$	$-\frac{1}{2}+y$	$\frac{1}{2}-z$
ii	$\frac{1}{2}+x$	$\frac{1}{2}-y$	-z	vii	$\frac{1}{2}+x$	$-\frac{1}{2}+y$	z
iii	-x	y	$\frac{1}{2}-z$	viii	$-\frac{1}{2}+x$	$\frac{1}{2}+y$	z
iv	1-x	y	$\frac{1}{2}-z$	ix	$-\frac{1}{2}-x$	$-\frac{1}{2}-y$	$-\frac{1}{2}+z$
v	$\frac{1}{2}-x$	$\frac{1}{2}+y$	$\frac{1}{2}-z$	x	x	-1+y	z
				xi	$-\frac{1}{2}+x$	$-\frac{1}{2}+y$	z

Table 25 (Continued)

O(W2)-O(3 ^{xi})	2.93(4)
O(W2)-O(5 ^{vi})	3.10(4)
O(W2)-O(6 ^x)	3.20(4)
O(W2)-O(14 ^{vii})	3.24(4)
O(W2)-Sb(2 ^{vi})	3.26(3)
O(W2)-Sb(2 ^{vii})	3.47(3)
O(W3)-O(14)	2.96(4)
O(W3)-O(5 ^{vii})	3.00(4)
O(W3)-O(W2)	3.14(5)
O(W3)-K(2 ^{vi})	3.15(3)
O(W3)-K(3 ^{iv})	2.68(3)

(b) Hydrogen bonding distances (Å) and angles (deg)

Donor	Hydrogen	Acceptor	O-O	Distances		O-H...O angle
				O-H	H...O	
O(W1)	H(W1a)	O(13 ^{vii})	3.04(2)	0.95	2.42	121
O(W1)	H(W1b)	O(16)	2.89(2)	0.94	1.95	172
O(W2)	H(W2a)	O(W1)	2.90(4)	0.83	2.31	129
O(W2)	H(W2b)	O(3 ^{xi})	2.93(4)	1.06	2.07	137
O(W3)	H(W3a)	O(15)	2.96(4)	1.04	2.06	144
O(W3)	H(W3a)	O(W2)	3.14(5)	0.90	2.60	112

The potassium atoms are situated between these layers and stabilize the solid via electrostatic interactions with tartrate and water oxygen atoms. Potassium-H₂O oxygen distances O(W1)-K(3^{vi}), O(W3)-K(2^{vi}), and O(W3)-K(3^{iv}): 2.76, 3.15, and 2.68Å, respectively, are comparable to K-O(H₂O) distances in K(Au(CN)₄)·H₂O⁶¹ and K(B₅O₆(OH)₄)·2H₂O.⁶² In addition, there are antimony-H₂O oxygen interactions, O(W2)-Sb(2^{vi}) and O(W2)-Sb(2^{vii}), 3.26 and 3.47Å, respectively. The latter distances are somewhat less than the sum of the van der Waal radii, 4.0Å,⁵⁹ and remind one of the Reihlen and Hezel structure where water occupies an antimony coordination site, but it is doubtful that this weak interaction would cause the water molecule to ionize in solution.

The coordination geometry of water oxygen atoms is not as clearly defined as in many other inorganic hydrate structures⁶³ where lone pair orbitals or the bisectrix of lone pair orbitals are directed toward metal atoms or are acceptors in hydrogen bonds. The potassium ions, in particular, do not necessarily occupy sp³ coordination sites on the H₂O oxygen atoms. O(W1), in addition to the two bonding atoms H(W1a) and H(W1b), is coordinated to K(3) and is also the acceptor atom in a hydrogen bond to O(W2). O(W2) is the donor atom in two hydrogen bonds and is the acceptor atom in a hydrogen bond with O(W3). It

is also weakly coordinated to Sb(2^{vi}) and Sb(2^{vii}). The third water molecule, O(W3), is coordinated to two potassium ions K(2^{vi}) and K(3^{iv}). Only one hydrogen atom in the third water molecule appears to be involved in hydrogen bonding, with bifurcated hydrogen bonds O(W3)-H(W3a)···O(11) and O(W3)-H(W3a)···O(W2).

RESEARCH PROPOSALS

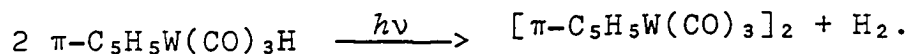
The following are problems in structural chemistry which could be solved by using X-ray and neutron diffraction techniques.

A. $\pi\text{-C}_5\text{H}_5\text{W}(\text{CO})_3\text{H}$ and $\pi\text{-C}_5\text{H}_5\text{Fe}(\text{CO})_3\text{PF}_6$

In an electron diffraction study of gaseous InC_5H_5 by Shibata, Bartell, and Gavin,⁶⁴ it was found that the hydrogen atoms are bent out of the plane of the carbon atoms away from the metal atom by $4.5 \pm 2^\circ$. This is due to the influence of the metal atom on orbital bonding in the ring.

A crystallographic study of π -cyclopentadienyl tricarbonyl tungsten hydride would be of interest to establish the coordination geometry about the tungsten atom, to determine the tungsten-hydrogen bond length, and to see if, in the solid state, the cyclopentadienyl hydrogen atoms lie in the plane of the carbon atoms, or whether they are bent out of the plane.

An X-ray structural investigation was carried out by Johnson in 1968,⁶⁵ and the results were poor (they were not published) due to rapid decomposition of the crystals when exposed to sunlight or artificial light. The crystals are pale yellow in color and change from yellow to dark red by the photodimerization reaction



A sample of this compound was supplied to me by R. J. Angelici. The crystals were mounted in thin-walled Lindemann capillaries to prevent decomposition. Preliminary precession photographs using Mo K α radiation were taken with a cardboard box over the camera to limit exposure to light. These photographs displayed 2/m Laue symmetry with extinctions $0k0: k \neq 2n$, which indicate the space groups $P2_1$ or $P2_1/m$.

The lattice constants from these photographs were $a=6.54$, $b=10.93$, $c=5.94\text{\AA}$, and $\beta=108.5^\circ$. The lattice constants in Johnson's thesis are $a=6.84$, $b=10.69$, $c=6.27\text{\AA}$, and $\beta=108.42^\circ$, which were determined by film techniques. The problems in refining the structure may have been due to using incorrect lattice constants.

A set of X-ray data for $\pi\text{-C}_5\text{H}_5\text{W}(\text{CO})_3\text{H}$ were taken in this laboratory with no appreciable decomposition of the crystal monitored by standard reflections measured periodically during data collection. The crystal was aligned optically on the diffractometer and the data were collected in the dark. Unfortunately, the data were not good enough for redetermining the crystal structure due to technical difficulties with the diffractometer. The tungsten atom positions (0.031, 0, 0.406) were located from an unsharpened Patterson map.

X-ray data could be retaken quite easily on this compound providing the overhead lights were off and the shades were drawn. A neutron diffraction study, however, would be the most interesting to locate the hydrogen atoms, and should be possible since the crystals do tend to grow to large size. For a white radiation neutron study, a large cardboard roof could be placed on top of the wall for biological shielding which presently surrounds the instrument.

A neutron diffraction study of $\pi\text{-C}_5\text{H}_5\text{Fe}(\text{CO})_3\text{PF}_6$ would also be interesting to see if the hydrogen atoms are pushed out of the plane of the cyclopentadienyl ring.

$\pi\text{-C}_5\text{H}_5\text{Fe}(\text{CO})_3^+$ has lower symmetry than InC_5H_5 and higher symmetry than $\pi\text{-C}_5\text{H}_5\text{W}(\text{CO})_3\text{H}$. If the hydrogen atoms are bent out of the plane, it would also be interesting to observe and compare the effect of the metal atom on individual hydrogen atoms in the lower symmetry cases.

B. Insecticides

Other cyclodiene insecticides which might be studied by X-ray diffraction are telodrin and heptachlor. The molecular parameters could then be compared to those of endrin, aldrin, and dieldrin. If crystals were available, the two forms of Klein's metabolite, the major metabolites of dieldrin and aldrin, would be especially interesting problems to solve using X-ray crystallography.

C. Studies of biologically important base pairs

In the Watson and Crick model of DNA, hydrogen bonds between the base pairs thymine-adenine and cytosine-guanine hold together the two polynucleotide helical chains. In the Watson and Crick model there are two hydrogen bonds between the base pairs, and in the later Pauling and Corey model there are three hydrogen bonds between guanine and cytosine.

Two X-ray structure determinations, 9-ethylguanine:1-methylcytosine⁶⁶ and 9-ethylguanine:1-methyl-5-bromocytosine,⁶⁷ have been reported. Although it is understood that hydrogen bonding between base pairs in nucleic acids is not necessarily the same as that found between isolated base pairs, the information obtained is useful for accurate model building. Neutron diffraction studies of these compounds would provide more accurate positional parameters and meaningful thermal parameters for hydrogen atoms in the crystal structures.

A series of purine-pyrimidine base pairs studies by Sobell using X-ray diffraction would also be interesting to redetermine using neutron diffraction if large enough crystals could be obtained. These are 9-ethyladenine:1-methyl-5-iodouracil, 1-methylthymine:9-ethyl-2,6-diaminopurine, and 1-methyl-5-uracil:9-ethyl-2-aminopurine.

REFERENCES

1. L. Busetto and R. J. Angelici, Inorg. Chim. Acta, 2, 391 (1968).
2. R. J. Angelici and L. Busetto, J. Amer. Chem. Soc., 91, 3197 (1969).
3. R. J. Angelici and L. J. Blacik, Inorg. Chem., 11, 1754 (1972), and references therein.
4. D. E. Williams, "LCR2: Fortran Lattice Constant Refinement Program," USAEC Report IS-1052, Ames Laboratory, Iowa State University, Ames, Iowa, 1967.
5. L. E. Alexander and G. S. Smith, Acta Cryst., 15, 983 (1962).
6. S. L. Lawton and R. A. Jacobson, Inorg. Chem., 7, 2124 (1968).
7. C. R. Hubbard, C. O. Quicksall and R. A. Jacobson, "The Fast Fourier Algorithm and the Programs ALFF, ALFFDP, ALFFPROJ, ALFFT, and FRIEDEL," USAEC Report IS-2625, Ames Laboratory, Iowa State University, Ames, Iowa, 1971.
8. W. R. Busing, K. O. Martin, and H. A. Levy, "OR FLS, A Fortran Crystallographic Least-Squares Program," USAEC Report ORNL-TM-305, Oak Ridge National Laboratory, Oak Ridge, Tennessee, 1962.
9. P. A. Doyle and P. S. Turner, Acta Cryst., A24, 390 (1968).
10. "International Tables for X-Ray Crystallography," Vol. III, 2nd ed., Kynoch Press, Birmingham, England, 1968, p. 215.
11. H. P. Hanson, F. Herman, J. D. Lea, and S. Skillman, Acta Cryst., 17, 1040 (1964).
12. W. R. Busing, K. O. Martin, and H. A. Levy, "OR FFE, A Fortran Crystallographic Function and Error Program," USAEC Report ORNL-TM-306, Oak Ridge National Laboratory, Oak Ridge, Tennessee, 1964.

13. C. K. Johnson, "OR TEP: A Fortran Thermal Ellipsoid Plot Program for Crystal Structure Illustrations," USAEC Report ORNL-3794, Oak Ridge National Laboratory, Oak Ridge, Tennessee, 1970.
14. F. A. Cotton, "Chemical Applications of Group Theory," 2nd ed., Wiley-Interscience, New York, N. Y., 1971, p. 236.
15. M. R. Churchill and J. Wormald, Inorg. Chem., 8, 1936 (1969).
16. M. R. Churchill and J. Wormald, J. Amer. Chem. Soc., 93, 354 (1971).
17. T. L. Brown and D. J. Darensbourg, Inorg. Chem., 6, 971 (1967).
18. S. F. A. Kettle, Inorg. Chem., 4, 1661 (1965).
19. L. F. Dahl and C. H. Wei, Inorg. Chem., 2, 713 (1963).
20. M. J. Bennett, M. R. Churchill, M. Gerloch, and R. Mason, Nature, 201, 1318 (1964).
21. M. Gerloch and R. Mason, J. Chem. Soc., 296 (1965).
22. A. F. Berndt and R. E. Marsh, Acta Cryst., 16, 118 (1963).
23. J. M. Coleman, A. Wojcicki, P. J. Pollick, and L. F. Dahl, Inorg. Chem., 6, 1236 (1967).
24. L. F. Dahl and N. G. Connelly, J. Amer. Chem. Soc., 92, 7472 (1970).
25. R. Mason and G. B. Robertson, J. Chem. Soc. A, 1229 (1970).
26. G. S. D. King, Acta Cryst., 15, 243 (1962).
27. P. J. Hansen and R. A. Jacobson, J. Organometal. Chem., 6, 389 (1966).
28. M. J. Bennett, F. A. Cotton, A. Davison, J. W. Faller, S. J. Lippard, and S. M. Morehouse, J. Amer. Chem. Soc., 88, 4371 (1966).

29. R. L. Metcalf, "Organic Insecticides," Interscience, New York, N. Y., 1955, pp. 233-248.
30. R. L. Metcalf, "Pesticides in the Environment," Vol. I, Part I, R. White-Stevens, Ed., Marcel Dekker, New York, N. Y., 1971, pp. 87-92.
31. S. B. Soloway, Advan. Pest Control Res., 6, 85 (1965).
32. D. E. H. Frear, "Pesticide Index," College Science Publishers, State College, Pa., 1969, pp. 156, 209.
33. P. G. Stecher, Ed., "Merck Index," Merck and Co., Rahway, N. J., 1968, pp. 356, 408-409.
34. W. T. Thomson, "Agricultural Chemicals," Simmons Publishing Co., Davis, Calif., 1964, pp. 22-25.
35. British Crop Protection Council, "Insecticide and Fungicide Handbook," Hubert Martin, Ed., Blackwell Scientific Publications, Oxford, England, 1969, pp. 353-354.
36. N. W. Alcock, presented in part at the International Summer School on Crystallographic Computing, Ottawa, Canada, August, 1969.
37. J. D. Scott, Queens University, Kingston, Ontario, Canada, personal communication, 1971.
38. P. Main, M. M. Woolfson, and G. Germain, "MULTAN, A Computer Program for the Automatic Solution of Crystal Structures," University of York, England, 1971.
39. J. Karle and H. A. Hauptman, Acta Cryst., 9, 635 (1956).
40. A. A. Khan, W. H. Baur, and M. A. Q. Khan, Acta Cryst., B28, 2060 (1972).
41. T. P. DeLacy and C. H. L. Kennard, J. Chem. Soc., Perkin II, 14, 2153 (1972).
42. J. N. Damico, J. T. Chen, C. E. Costello, and E. O. Haenni, J. Ass. Offic. Anal. Chem., 51, 48 (1968).
43. W. R. Benson, J. Ass. Offic. Anal. Chem., 52, 1109 (1969).

44. R. C. Weast, Ed., "Handbook of Chemistry and Physics," Chemical Rubber Co., Cleveland, Ohio, 1970, pp. B-121, C-270.
45. J. E. Johnson and R. A. Jacobson, Acta Cryst., in press.
46. B. Kamenar, D. Grdenić, and C. K. Prout, Acta Cryst., B26, 181 (1970).
47. G. A. Kiosse, N. I. Golovastikov, A. V. Ablov, and N. V. Belov, Doklady Akad. Nauk SSSR, 177, 329 (1967) [Soviet Physics-Doklady, 12, 990 (1968)].
48. Hsiang-Ch'i Mu, K'o Hseuh T'ung Pao, 17, 502 (1966).
49. H. Reihlen and E. Hezel, Ann. Chem., 487, 213 (1931).
50. G. A. Kiosse, N. I. Golovastikov, and N. V. Belov, Kristallografiya, 9, 402 (1964) [Soviet Physics - Crystallography, 9, 321 (1964)].
51. C. R. Hubbard, C. O. Quicksall, and R. A. Jacobson, Acta Cryst., A28, 236 (1972).
52. C. R. Hubbard, C. O. Quicksall, and R. A. Jacobson, Acta Cryst., in press.
53. G. E. Bacon, "Neutron Diffraction," Oxford Univ. Press, Oxford, 1962, pp. 31, 61.
54. Neutron Diffraction Commission, Acta Cryst., A25, 391 (1969).
55. R. E. Tapscott, R. L. Belford, and I. C. Paul, Coordin. Chem. Rev., 4, 323 (1969).
56. J. E. Griffiths, R. P. Carter, Jr., and J. R. Holmes, J. Chem. Phys., 41, 863 (1964).
57. L. S. Bartell and K. W. Hansen, Inorg. Chem., 4, 1777 (1965).
58. D. R. Schroeder and R. A. Jacobson, Inorg. Chem., 12, 210 (1973), and references therein.
59. L. Pauling, "The Nature of the Chemical Bond," Cornell University Press, Ithaca, N. Y., 1960, p. 260.

60. W. C. Hamilton and J. A. Ibers, "Hydrogen Bonding in Solids," W. A. Benjamin, New York, N. Y., 1968, p. 204.
61. C. Bertinotti and A. Bertinotti, Acta Cryst., B26, 422 (1970).
62. J. P. Ashmore and H. E. Petch, Canad. J. Phys., 47, 1091 (1969).
63. G. Ferraris and M. Franchini-Angela, Acta Cryst., B28, 3572 (1972).
64. S. Shibata, L. S. Bartell, and R. M. Gavin, Jr., J. Chem. Phys., 41, 717 (1964).
65. P. L. Johnson, Ph.D. Thesis, Washington State University, Pullman, Washington, 1968.
66. E. J. O'Brien, J. Mol. Biol., 7, 107 (1963).
67. H. M. Sobell, K. Tomita, and A. Rich, Proc. Nat. Acad. Sci., 49, 885 (1963).

ACKNOWLEDGEMENTS

I would like to express my sincere appreciation
to:

Professor R. A. Jacobson, for his generous
assistance and guidance in my work, and for
his confidence in me as an individual;
Professors R. J. Angelici and P. A. Dahm, for the
suggestion of and helpful discussions
concerning the iron carbonyl and insecticide
problems;
C. R. Hubbard, whose assistance was invaluable in
starting the first research projects;
M. L. Hackert, C. O. Quicksall, J. E. Benson,
H. F. Hollenbeck, and other members of X-Ray
Group I;
H. E. Wright, for helpful discussions about
organic chemistry;
and to my parents, Byron Edward and Grace Dotson
Gress, for their continued support and
encouragement.